

SUPPLEMENTAL MATERIAL

Type 1 angiotensin receptors on macrophages ameliorate IL-1 receptor-mediated kidney fibrosis

Jian-dong Zhang¹, Mehul B. Patel¹, Robert Griffiths¹, Paul C. Dolber³, Phillip Ruiz⁵, Matthew A. Sparks¹, Johannes Stegbauer⁶, Huixia Jin¹, Jose A. Gomez², Anne F. Buckley⁴, William S. Lefler¹, Daian Chen¹, and Steven D. Crowley¹

¹Division of Nephrology and ²Cardiology, Departments of Medicine, ³Surgery, and ⁴Pathology, Durham VA and Duke University Medical Centers, Durham, North Carolina, USA. ⁵Department of Pathology, University of Miami, Miami, Florida, USA. ⁶Department of Nephrology, Medical Faculty, Heinrich-Heine University Düsseldorf, Düsseldorf, Germany.

Corresponding Author: Steven D. Crowley, Box 103015 DUMC, Durham, NC 27710, Phone: 919-684-9788. Fax 919-684-3011. E-mail: steven.d.crowley@duke.edu

Additional Results and Discussion

Supplemental Paragraph 1: Generation of mice with deletion of the AT_{1A} receptor on myeloid cells. As the AT_{1A} receptor is the dominant murine AT₁ receptor isoform and the functional homolog to the human AT₁ receptor, we examined the functions of the AT₁ receptor on macrophages in mice by removing AT_{1A} receptor-mediated responses specifically from myeloid cells via a *Cre-Lox* gene targeting approach. The Lysozyme-M (*LysM*) promoter is exclusively active in hematopoietic cells of myelomonocytic lineage and is highly expressed in mature macrophages (1). By breeding a *LysM-Cre* mouse line with a double fluorescence reporter mouse (*mT/mG*) (2), we confirmed recombinant *Cre* expression marked by GFP within the spleen and peritoneal macrophages of *LysM-Cre⁺ mT/mG* mice but the absence of *Cre* expression marked by red fluorescent protein in nonlymphoid tissues such as the kidney (Supplemental Figure S1). We therefore bred *LysM-Cre* mice with an *Agtr1a flox* line, yielding *LysM-Cre⁺ Agtr1a^{flox/flox}* mice (*Macro KO*) and *LysM-Cre⁻ Agtr1a^{flox/flox}* (*WT*) littermates for our experiments. We then isolated F4/80⁺ macrophages (Supplemental Figure S2), CD3⁺ T lymphocytes, CD19⁺ B cells, kidney, and heart in order to characterize AT_{1A} receptor expression in the tissues of the *Macro KO* mice. Using real-time qPCR, we noted a 75% reduction in AT_{1A} receptor expression in F4/80⁺ macrophages from *Macro KO* mice compared with their *WT* littermates but preserved AT_{1A} receptor expression in all other tissues examined (Supplemental Figure S3). In primary cultures of macrophages from the *Macro KO* animals, we further detected a > 95% AT_{1A} receptor deletion (Supplemental Figure S4) but no expression of the alternate AT_{1B} receptor isoform (data not shown).

S1

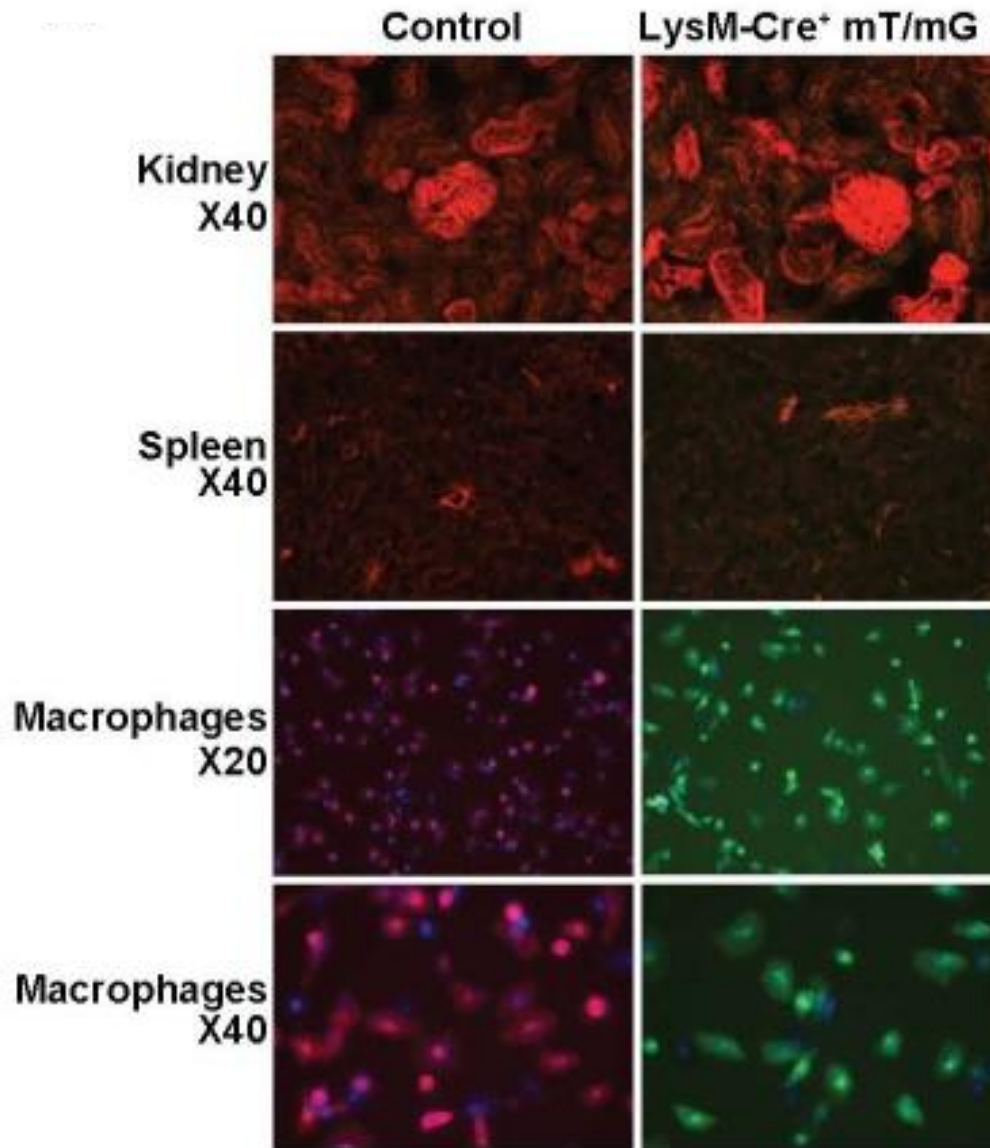
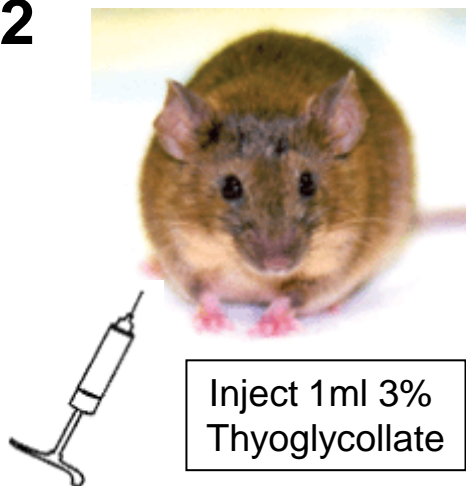
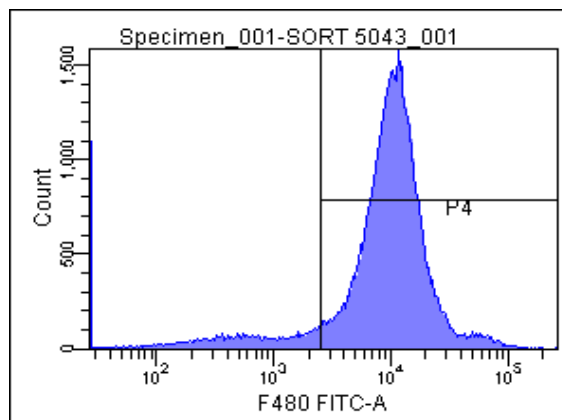
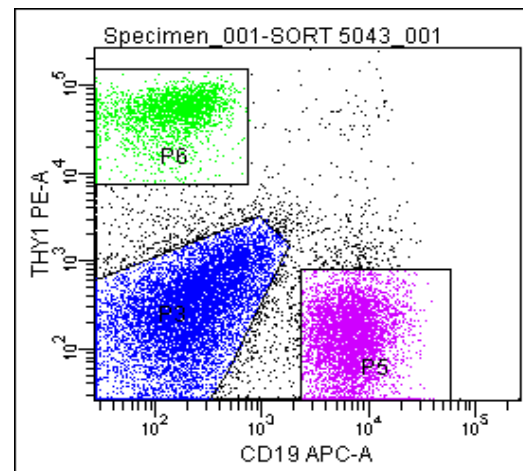


Figure S1. Verification of macrophage-specific *Cre* expression in *LysM-Cre* reporter mice. Representative images of kidney, spleen, and purified peritoneal macrophages in *LysM-Cre*⁺ *mT/mG* and control (*LysM-Cre*⁻ *mT/mG*) mice. Green fluorescence indicates the presence of *LysM-Cre* expression whereas red fluorescence indicates the absence of *LysM-Cre* expression. Blue fluorescence in macrophages is a nuclear DAPI stain.

S2

Wait 4 days for induction of peritoneal inflammation. Then, harvest and label peritoneal mononuclear cells



F4/80⁺ Thy1⁻ CD19⁻ **(Macrophages)**

Figure S2. Isolation of peritoneal macrophages for verification of AT_{1A} receptor deletion. Before embarking on experiments with the *Macro KO* animals, we first verified cell-specific deletion of the AT_{1A} receptor by purifying immune cell populations using fluorescent cell sorting strategies. For example, to purify macrophages, we injected mice intraperitoneally with thioglycollate and 4 days later harvested mononuclear cells from the peritoneal cavity. Then, we labeled and sorted the cells to isolate those cells expressing the macrophage marker F4/80 but not the T or B lymphocyte markers, Thy1.1 or CD19, respectively.

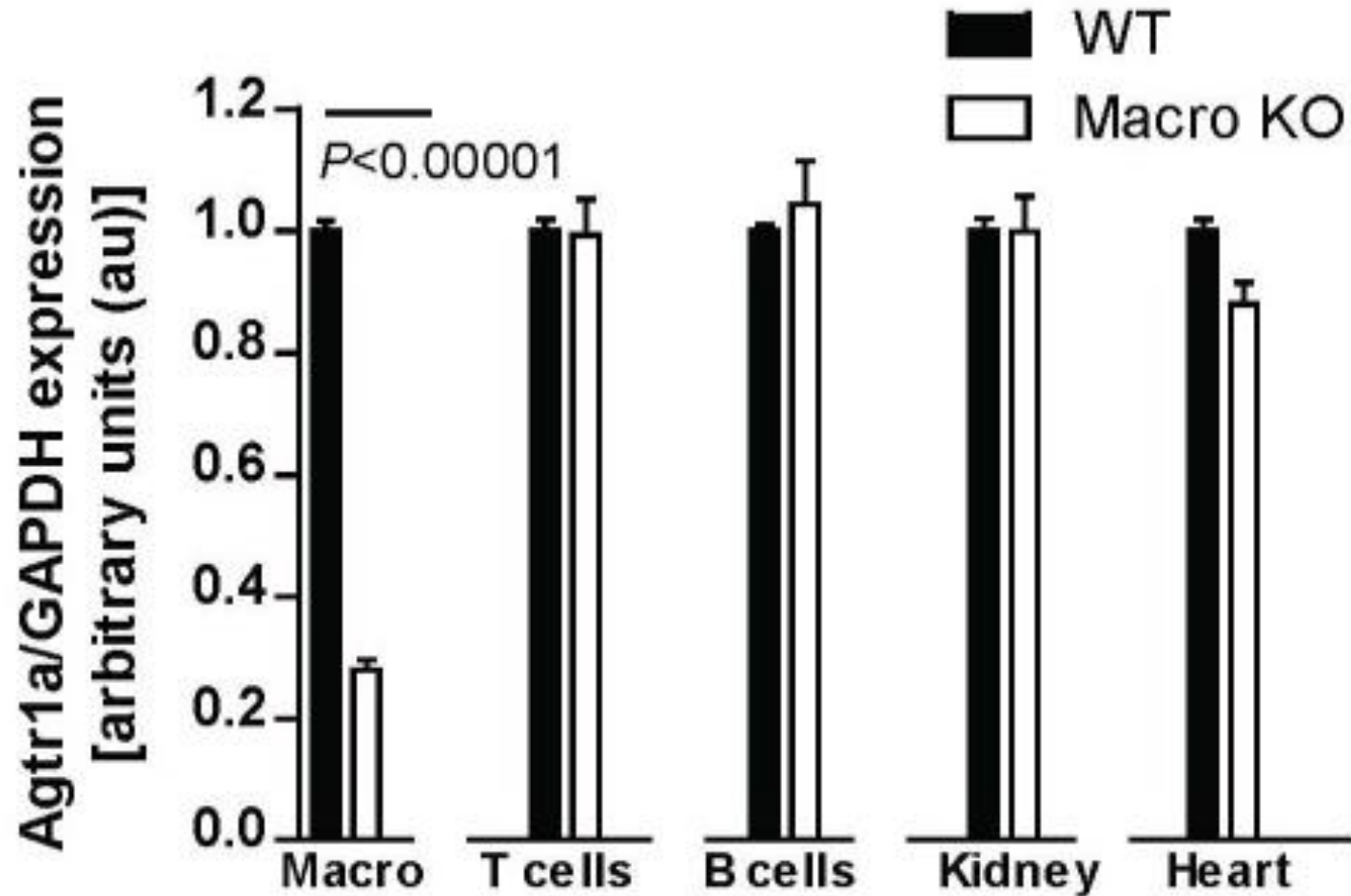


Figure S3. Verification of macrophage-specific deletion of the AT_{1A} angiotensin receptor in *Macro KO* mice. mRNA expression for the AT_{1A} receptor in isolated peritoneal macrophages (“Macro”), T cells, B cells, and in whole kidney and heart from *WT* and *Macro KO* animals.

S4

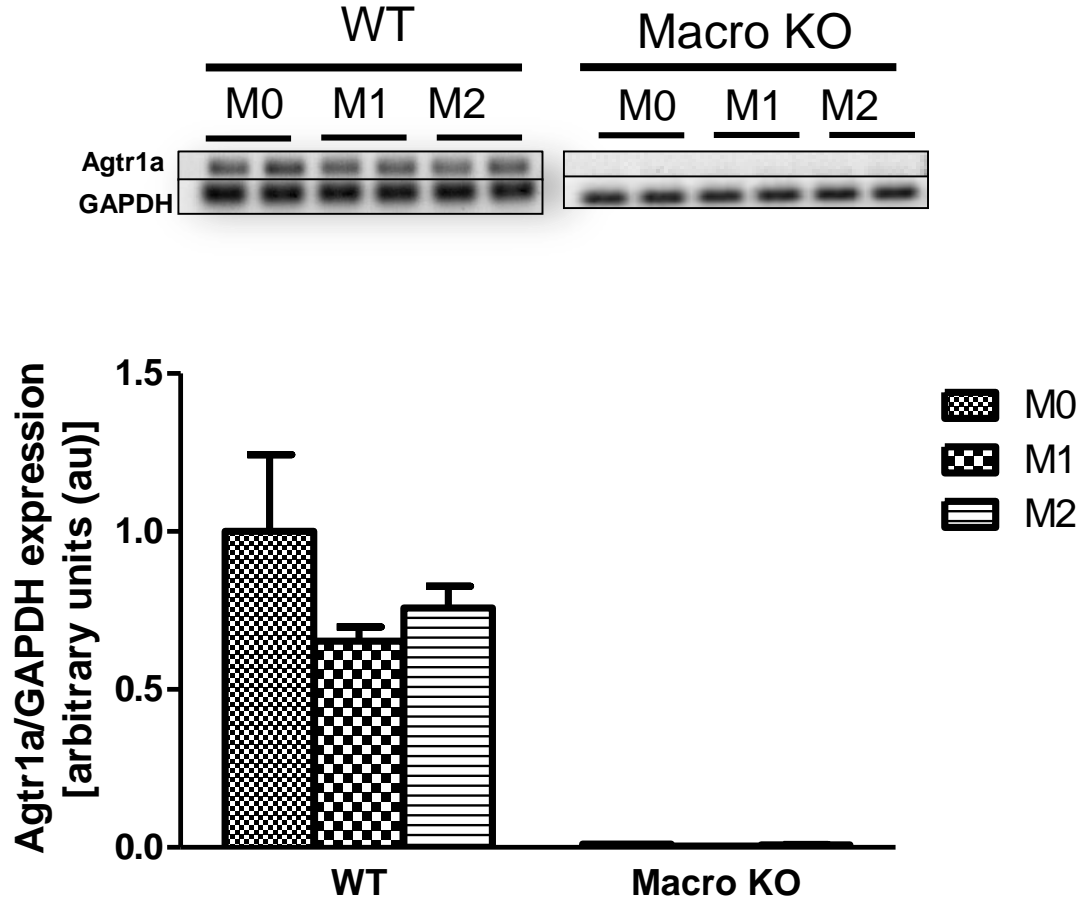


Figure S4. *Agtr1a* expression in cultured macrophages. mRNA expression for AT_{1A} receptor measured by RT-PCR in cultured resting (“M0”), M1-polarized (“M1”), or M2-polarized (“M2”) macrophages with representative bands on top and summary data on bottom.

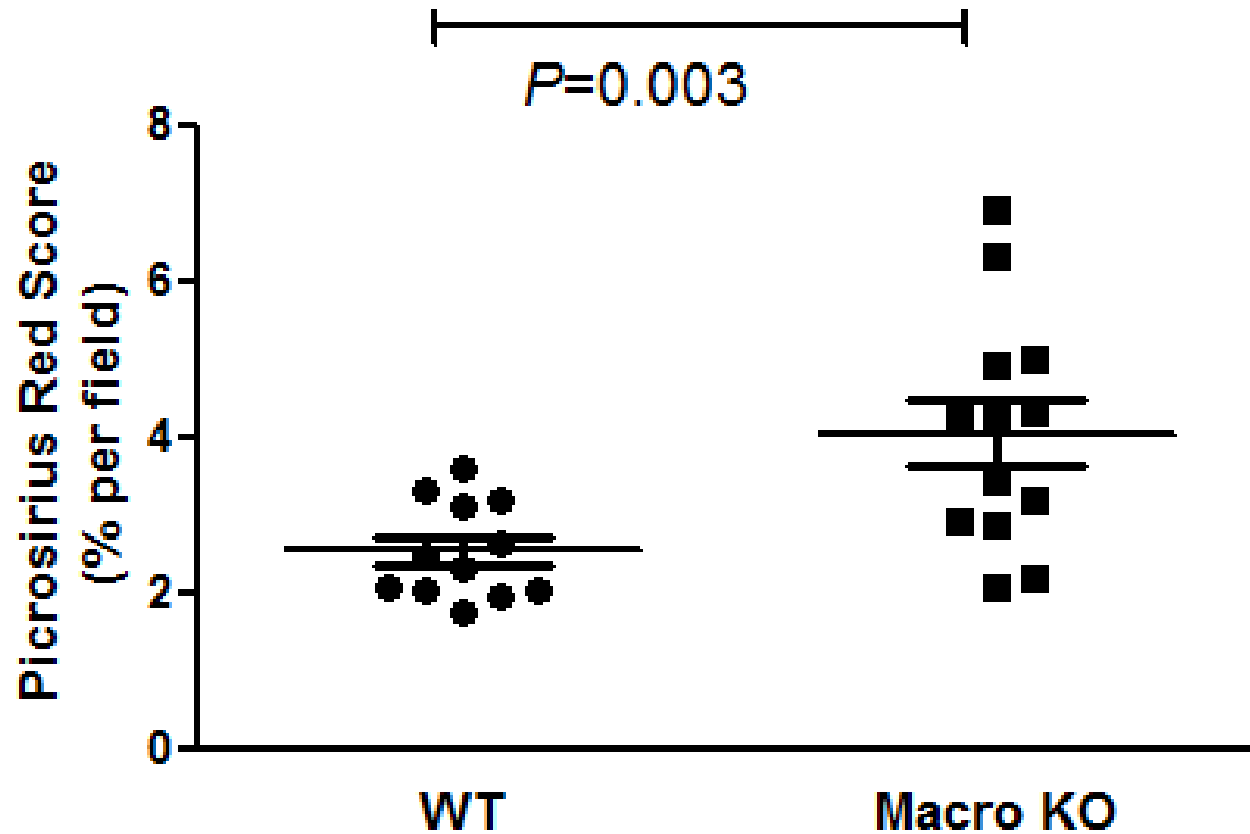


Figure S5. AT_{1A} receptor-deficiency on macrophages exacerbates kidney fibrosis induced by unilateral ureteral obstruction (UUO). Blinded morphometric quantitation of picrosirius red staining for collagen fibrils in obstructed *WT* and *Macro KO* kidneys after 7 days of UUO ($n \geq 12$ per group, representative images in Figure 1B of the main text).

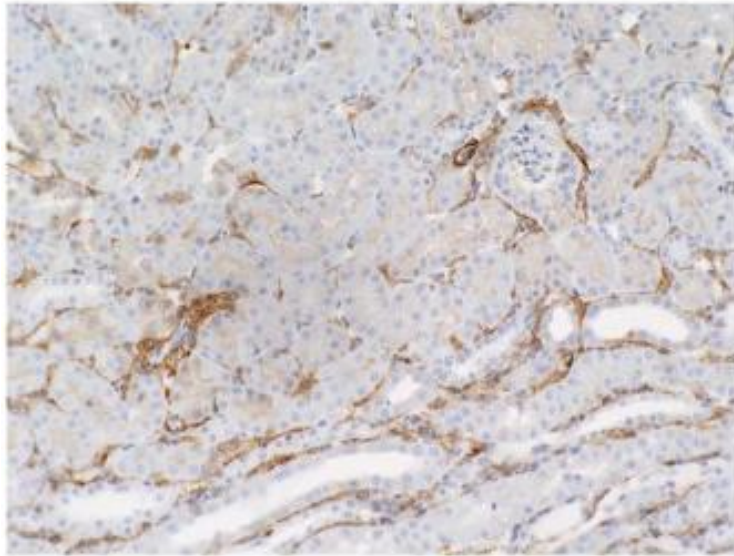
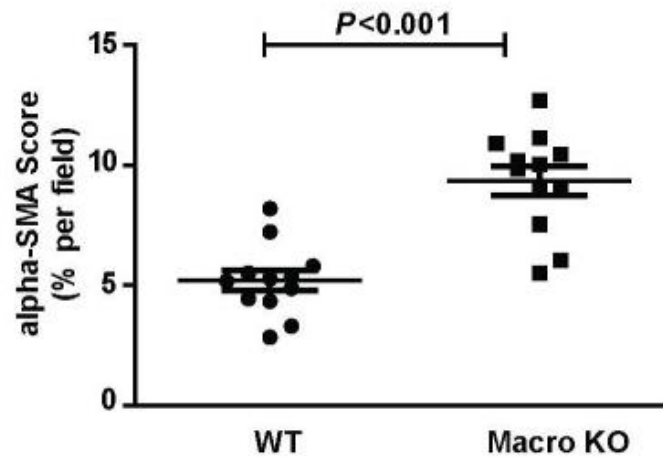
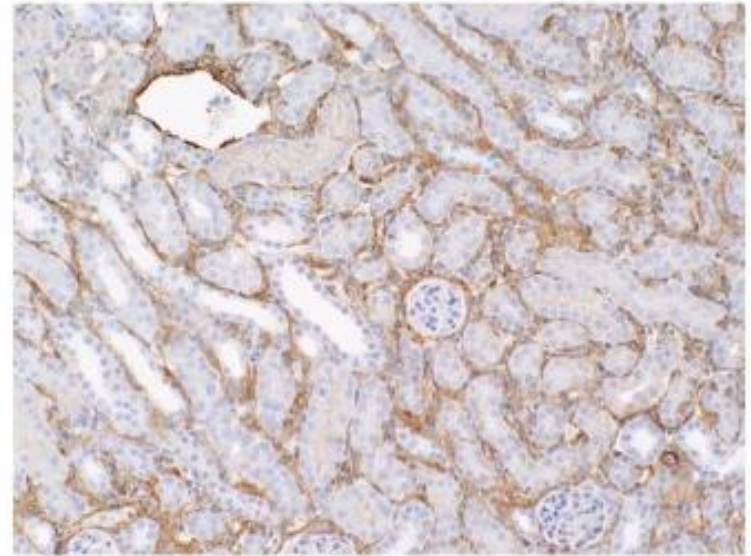
S6**WT****Macro KO**

Figure S6. Enhanced numbers of myofibroblasts in obstructed *Macro KO* kidneys. Top, representative sections from obstructed *WT* and *Macro KO* kidneys stained with α -smooth muscle actin for collagen-producing myofibroblasts at day 7 UOU. Bottom, blinded morphometric quantitation. (magnification X20)

Supplemental Paragraph 2: *Confirming the reno-protective actions of the macrophage AT₁ receptor.* Treatment of the *WT* and *Macro KO* animals with the AT₁ receptor antagonist losartan during the 7 days following UJO further confirmed the protective actions of the macrophage AT₁ receptor in this model. In this experiment, one might predict that the efficacy of losartan in the *WT* group would be blunted compared to the *Macro KO* group due to the blockade of protective signaling via the macrophage AT₁ receptor in the *WT* group that was already absent in the *Macro KO* animals without losartan treatment. Indeed, blockade of the renal AT₁ receptor in the *Macro KO* animals with losartan reduced collagen I deposition in the obstructed kidney considerably more than blocking both the renal and macrophage AT₁ receptors in the *WT* group, resulting in similar levels of residual renal fibrosis in the 2 groups (Supplemental Figure S7, left panels). Conversely, the presence of persistent, measurable fibrosis in the obstructed kidneys from both losartan-treated groups compared to the contralateral unobstructed kidneys illustrates the capacity for additional benefit from preserving AT₁ receptor signals on macrophages during the progression of kidney fibrosis (Supplemental Figure S7, right panels). Separately, using the Ang II-induced hypertension model in which tubular damage is a more prominent feature than fibrosis, we confirmed that kidneys from *Macro KO* mice displayed more severe injury than *WT* controls [5.9 ± 0.5 vs. 4.5 ± 0.5 arbitrary units (au); $P = 0.05$] despite a similar level of blood pressure elevation in the 2 groups (Supplemental Figure S8). These additional studies confirm that AT₁ receptor stimulation on macrophages infiltrating the kidney reduces progressive renal fibrosis and injury.

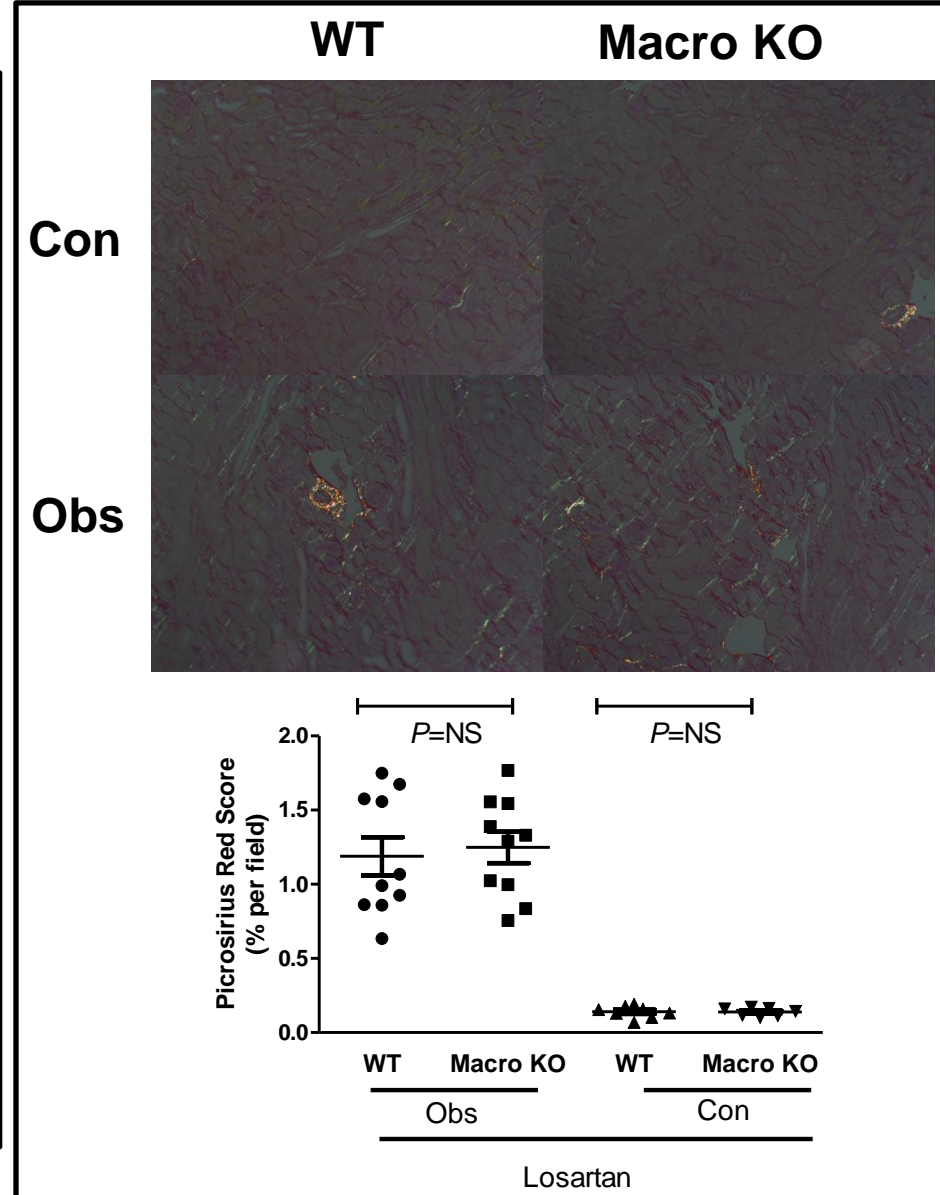
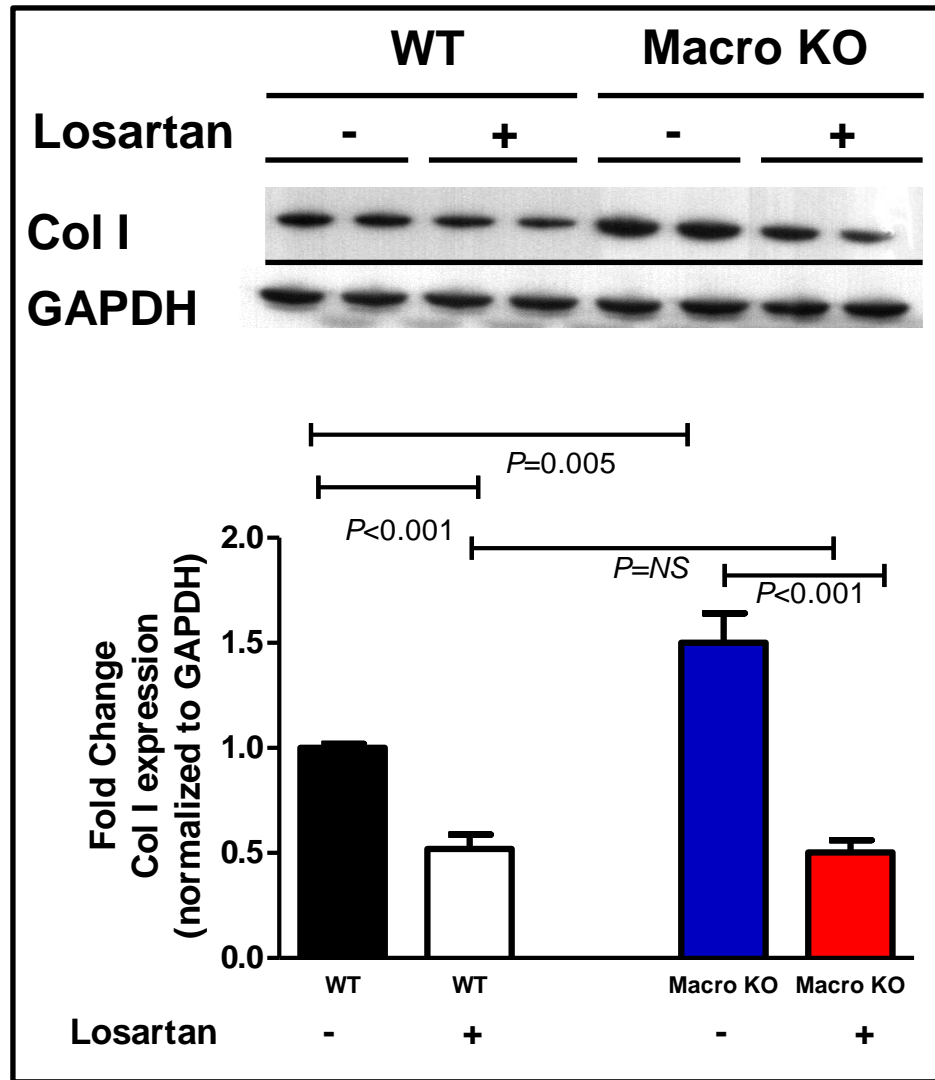
S7

Figure S7. AT₁ receptor blockade with losartan reduces UUO kidney fibrosis more in Macro KOs than WTs. Experimental animals were treated with losartan for 7 days following UUO. On left, western blot for collagen I (“Col I”) shows that losartan reduced renal collagen content more effectively in the *Macro KO* than in the *WT* obstructed kidneys. On right, picrosirius red staining of obstructed (“Obs”) and contralateral (“Con”) nonobstructed kidneys (n=7-10 per group) shows persistent and similar levels of fibrosis in the obstructed kidneys from both groups compared to contralateral controls. Representative images on top (X20). Summary data on bottom.

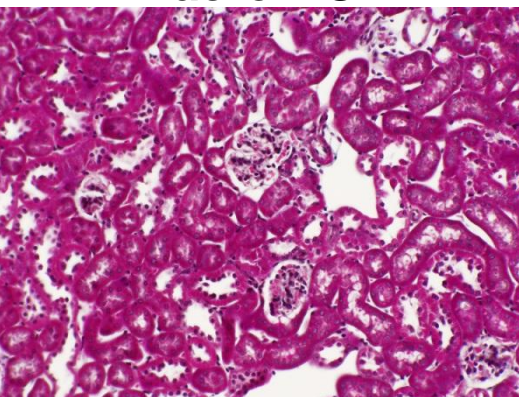
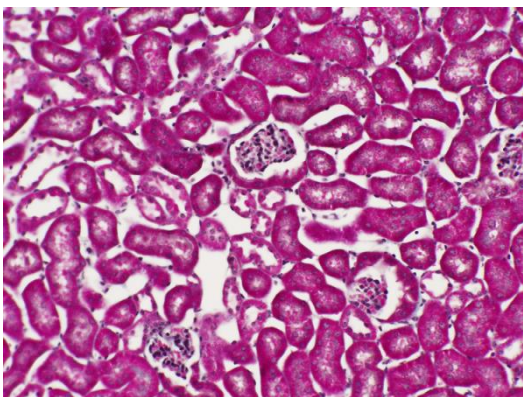
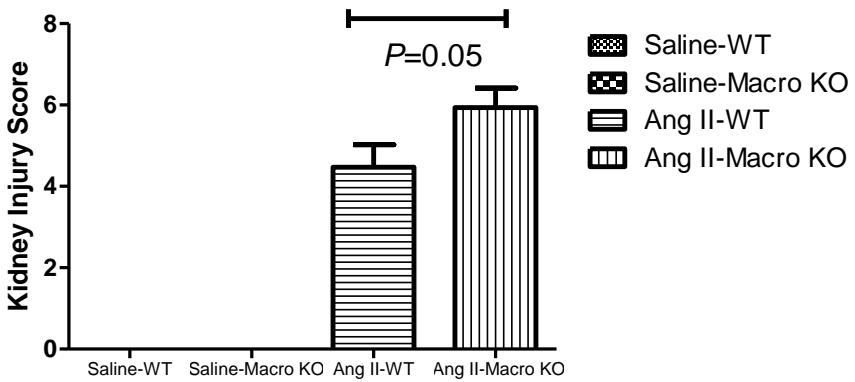
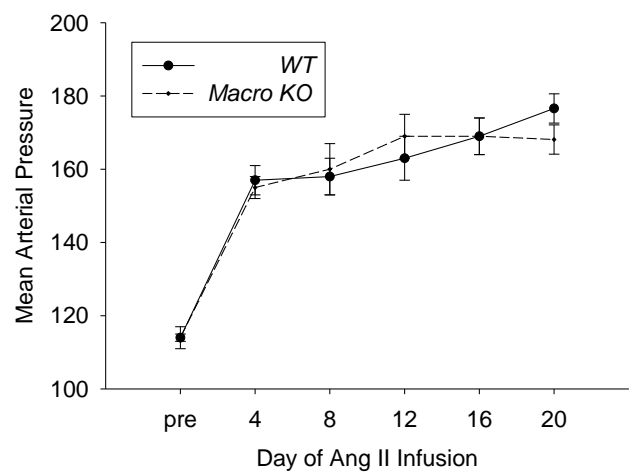
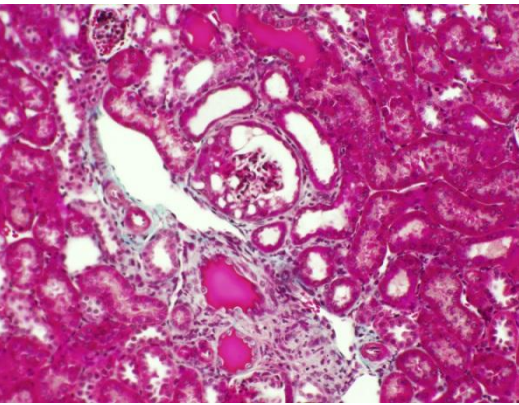
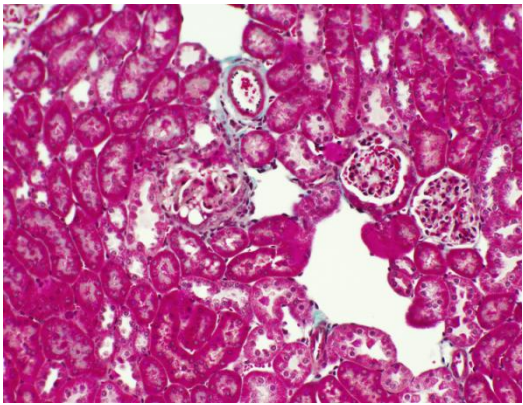
S8**WT****Macro KO****Saline****Ang II**

Figure S8. The macrophage AT₁ receptor protects against kidney damage induced by chronic angiotensin II infusion. Blinded scoring for kidney damage in uni-nephrectomized *WT* or *Macro KO* mice infused with saline or angiotensin II (“Ang II”) for 4 weeks revealed exaggerated injury in *Macro KO* kidneys following Ang II despite similar increases in blood pressure versus Ang II-infused *WT* controls. Representative images above (X20). Blood pressures in Ang II-infused groups on right.

Supplemental Paragraph 3: *Macrophage infiltration into the obstructed kidneys as assessed by histologic stains.* The enhanced expression of M1 cytokines in the obstructed *Macro KO* kidneys could accrue from increased accumulation of AT_{1A} receptor-deficient macrophages in the injured kidney and/or from effects of AT_{1A} receptor activation on the polarization of macrophages infiltrating the obstructed kidney. To test the first possibility, we stained the kidney sections with the macrophage marker F4/80 (Supplemental Figure S9). While there were increased numbers of F4/80⁺ macrophages in the *Macro KO* kidneys compared to *WT* controls at day 7 after UUO, this difference did not achieve statistical significance. Immunofluorescence staining of frozen sections similarly revealed a non-significantly higher number of iNOS⁺ M1 macrophages in the *Macro KO* kidneys dispersed throughout the renal interstitium but sparse and similar numbers of CD206⁺ M2 macrophages in the 2 groups (Supplemental Figure S10).

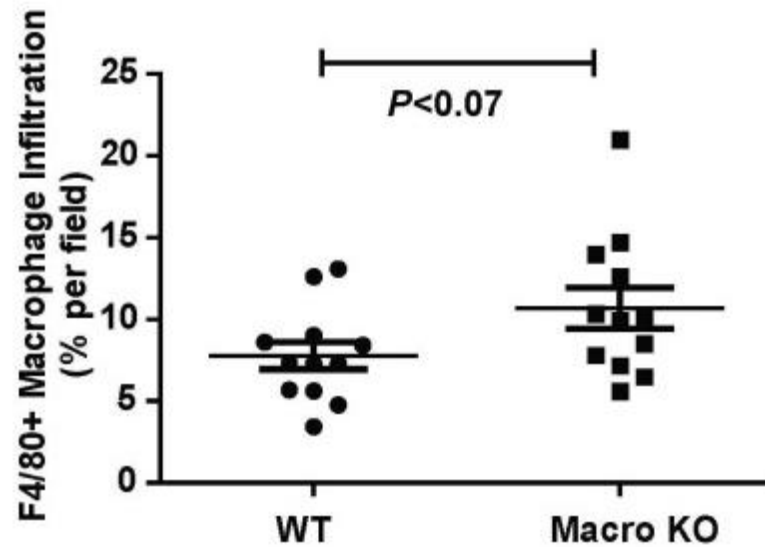
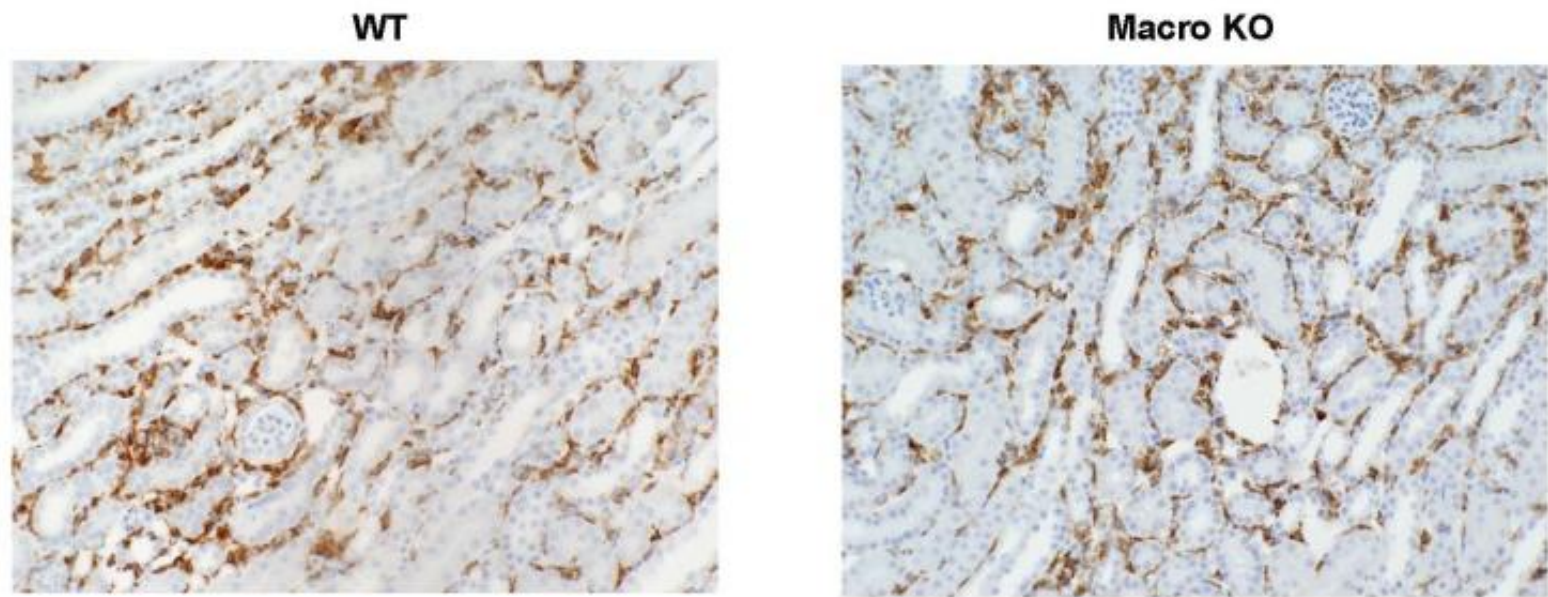
S9

Figure S9. Macrophage infiltration into WT and Macro KO kidneys following UUO. Top, representative sections showing F4/80+ macrophage infiltration in obstructed kidneys from WT and Macro KO mice at day 7 UUO. Bottom, blinded morphometric quantitation of F4/80 staining. (n≥12 per group)

S10A – F4/80⁺ iNOS⁺ Macrophages, x20

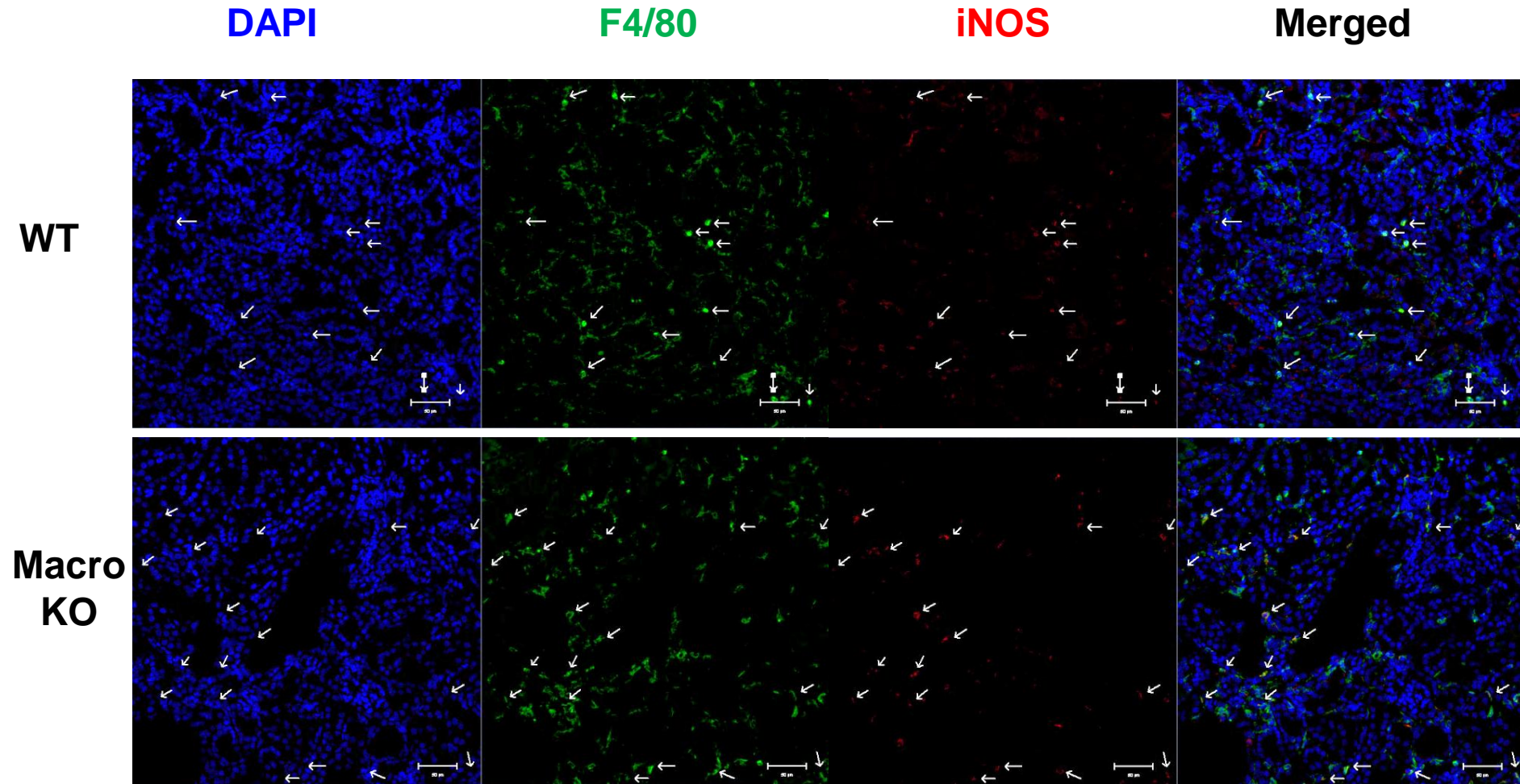


Figure S10. Infiltration of F4/80⁺ macrophages into kidney at day 7 UUO. (A) Representative frozen sections of obstructed kidney stained for DAPI (blue), F4/80⁺ (green), and iNOS (red) as an M1 macrophage marker. Stains presented separately and then merged via confocal microscopy. Arrows mark cells double positive for F4/80 and iNOS. (20X, scale bar = 50 microns)

S10B – F4/80⁺ iNOS⁺ Macrophages, x40

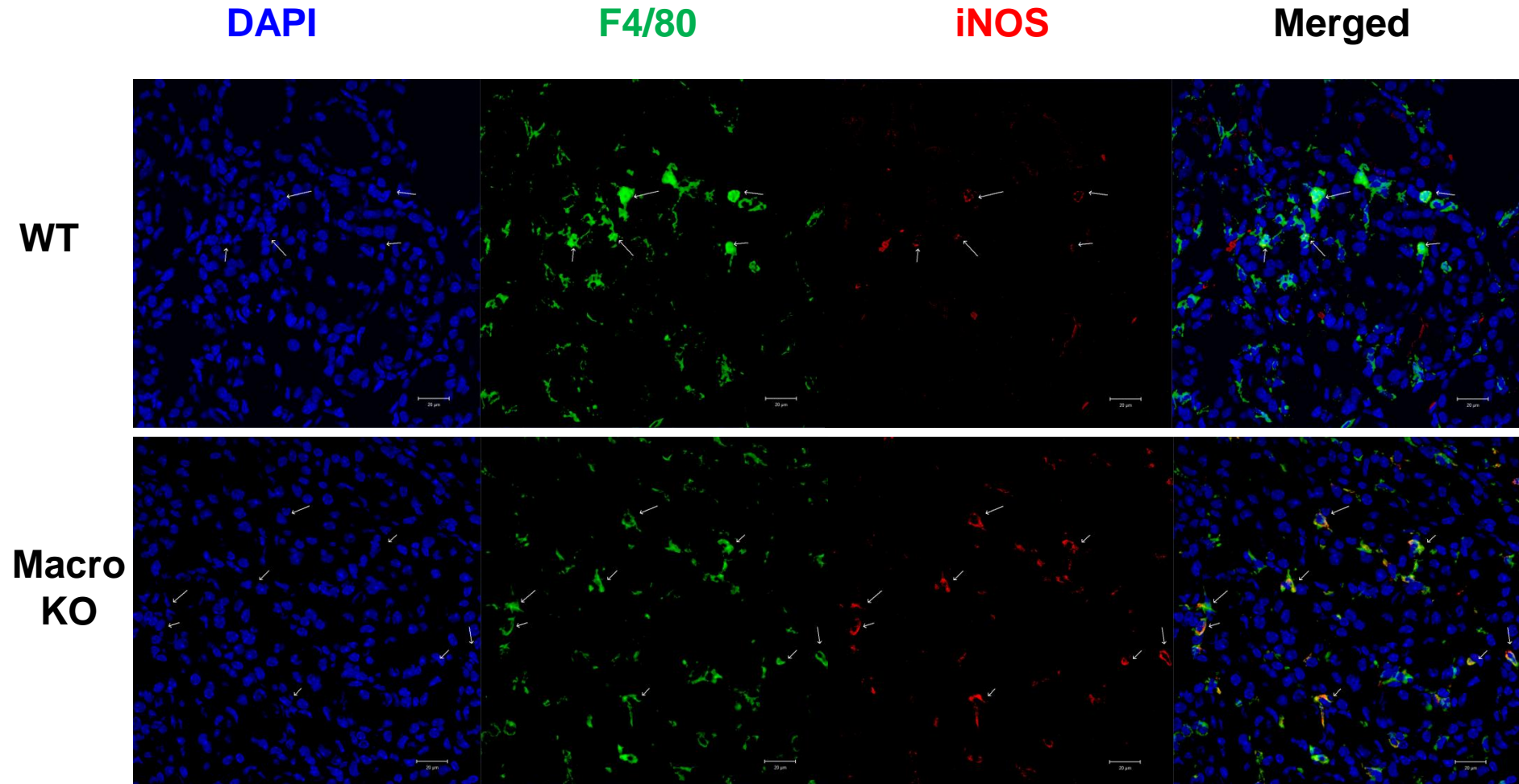


Figure S10. Infiltration of F4/80⁺ macrophages into kidney at day 7 UUO. (B) Representative frozen sections of obstructed kidney stained for DAPI (blue), F4/80⁺ (green), and iNOS (red) as an M1 macrophage marker. Arrows mark cells double positive for F4/80 and iNOS. (40X, scale bar = 20 microns)

S10C – F4/80⁺ CD206⁺ Macrophages, x20

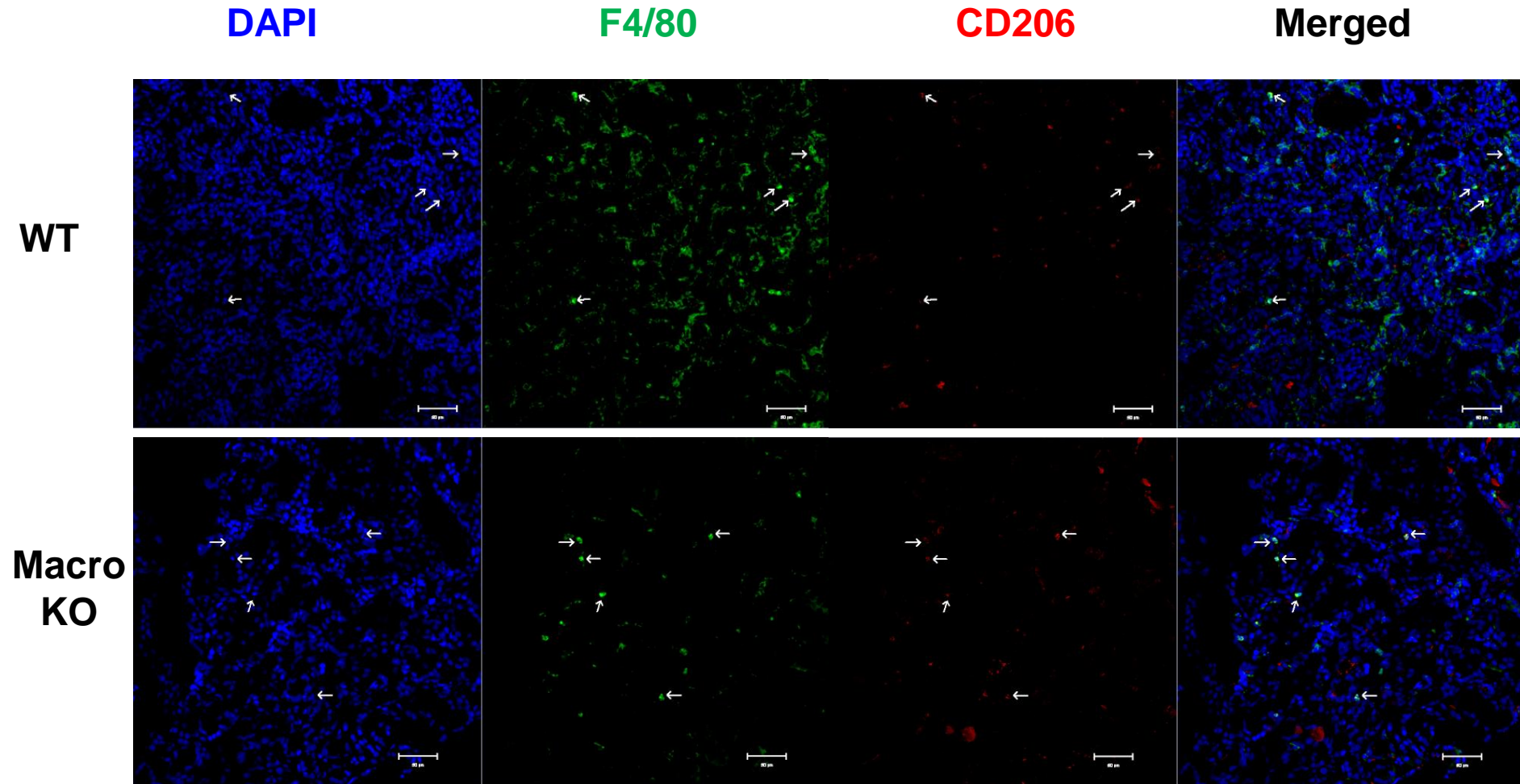


Figure S10. Infiltration of F4/80⁺ macrophages into kidney at day 7 UUO. (C) Representative frozen sections of obstructed kidney stained for DAPI (blue), F4/80⁺ (green), and the mannose receptor CD206 (red) as an M2 macrophage marker. Arrows mark cells double positive for F4/80 and CD206. (20X, scale bar = 50 microns)

S10D – F4/80⁺ CD206⁺ Macrophages, x40

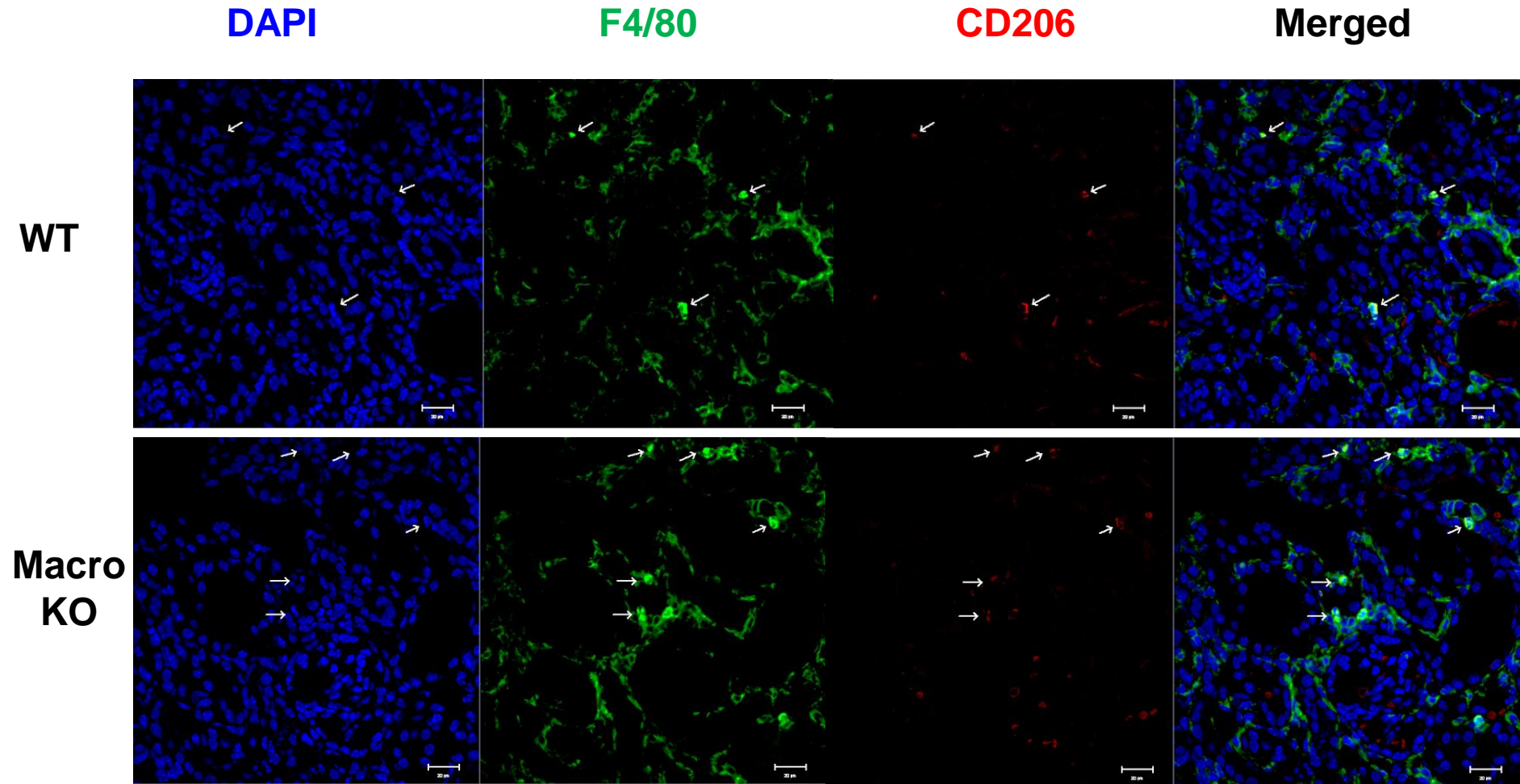


Figure S10. Infiltration of F4/80⁺ macrophages into kidney at day 7 UUO. (D) Representative frozen sections of obstructed kidney stained for DAPI (blue), F4/80⁺ (green), and the mannose receptor CD206 (red) as an M2 macrophage marker. Arrows mark cells double positive for F4/80 and CD206. (40X, scale bar = 20 microns)

S10E

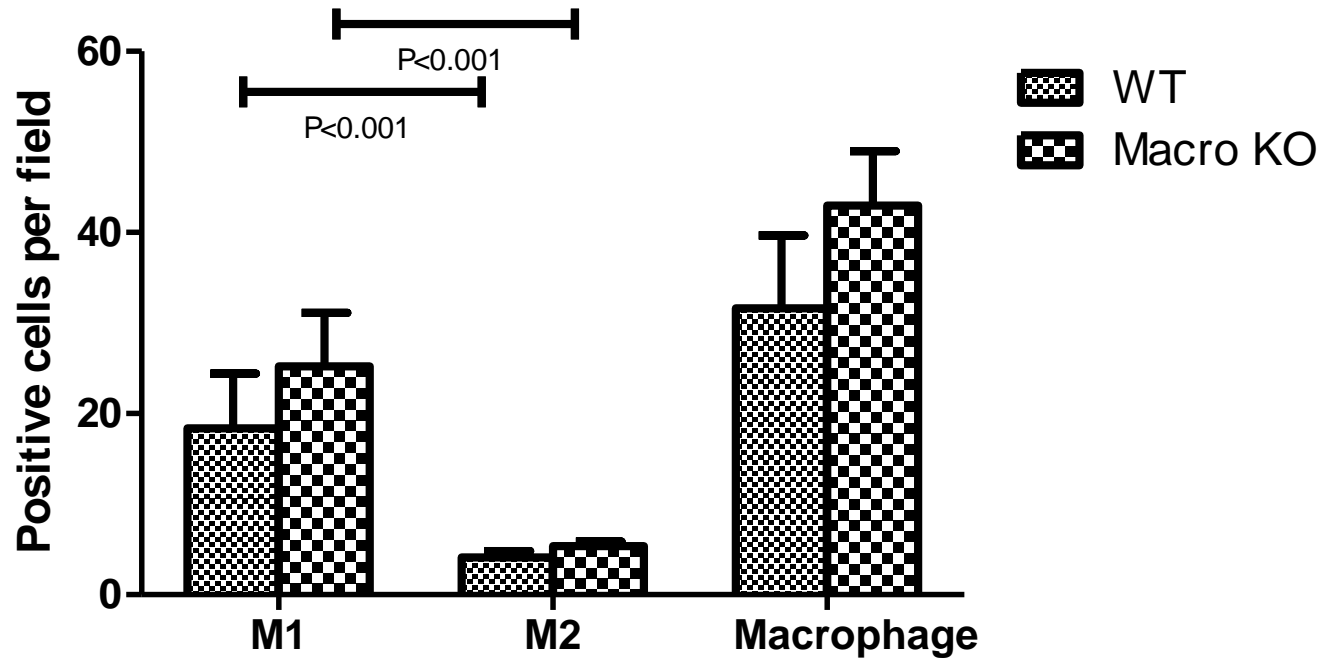
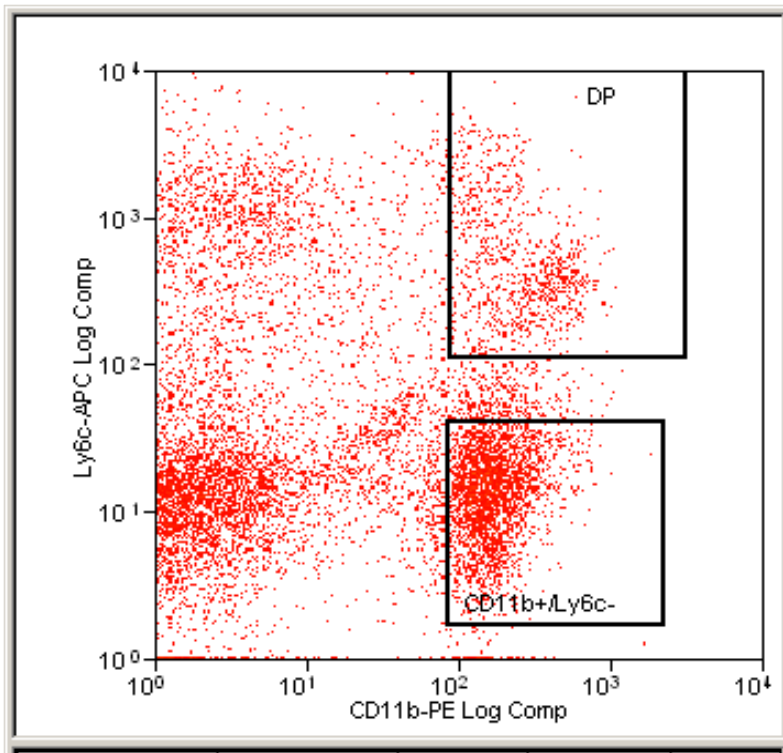
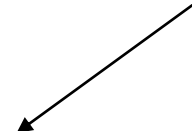
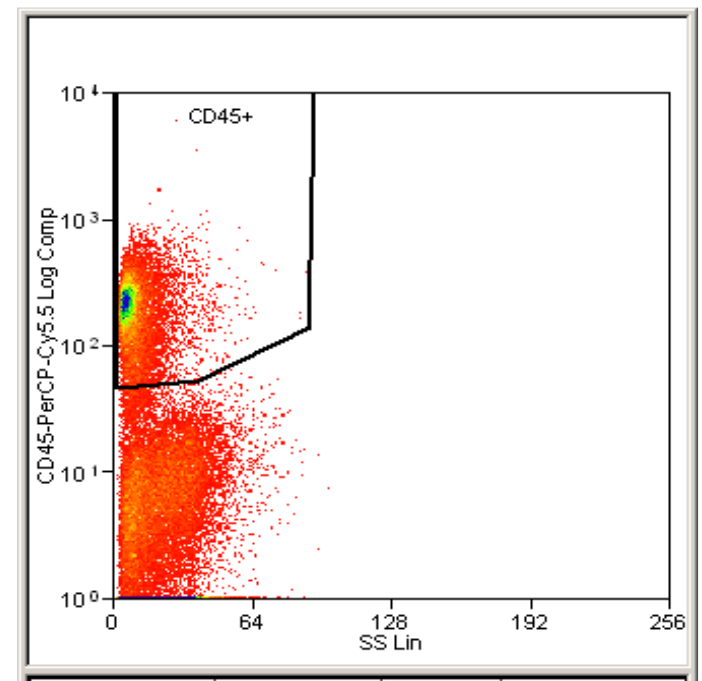


Figure S10. Infiltration of F4/80⁺ macrophages into kidney at day 7 UUO. (E) Quantitation of iNOS⁺ (“M1”) and CD206⁺ (“M2”) F4/80⁺ macrophages (n=4 per group) at 20X. M1 macrophages greatly outnumbered M2 macrophages in the renal interstitium based on these markers. Number of iNOS⁺ macrophages trended higher in obstructed *Macro KO* kidneys compared to *WTs*.

S11



After mincing, kidney tissues were incubated with collagenase and filtered through a 40 micron strainer. Single-cell suspensions were then fluorescently labeled.



CD45⁺ CD11b⁺ Ly6C^{hi}

CD45⁺ CD11b⁺ Ly6C^{lo}

Figure S11. Workflow for purifying activated macrophages directly from kidney. Obstructed kidneys were harvested at day 7 UUO, minced, digested, filtered to single cell suspensions, and labeled via a sequential gating strategy to allow fluorescent cell sorting: anti-CD45 for mononuclear cells, CD11b for myeloid cells, and Ly6C for infiltrating activated macrophages. Gene expression for inflammatory mediators was then analyzed in these cells via real-time RT-PCR.

Supplemental Paragraph 4: *Confirming the propensity of AT₁ receptor-deficient macrophages toward M1 differentiation.* We confirmed that AT_{1A} receptor-deficient macrophages had exaggerated cytokine production following M1 stimulation by measuring the contents of IL-1 β and CCL5 proteins in the supernatants of the macrophage culture media (Supplemental Figure S12). By contrast, M2 polarization of *WT* and *Macro KO* macrophages caused robust and similar mRNA induction of the M2 markers FIZZ1 and YM-1 (Supplemental Figure S13) and the secreted cytokine IL-10 (1.00 \pm 0.22 vs. 0.93 \pm 0.17 au; *P* = NS). Thus, AT₁ receptor activation on macrophages suppresses their M1 differentiation without influencing their susceptibility to M2 polarization.

S12

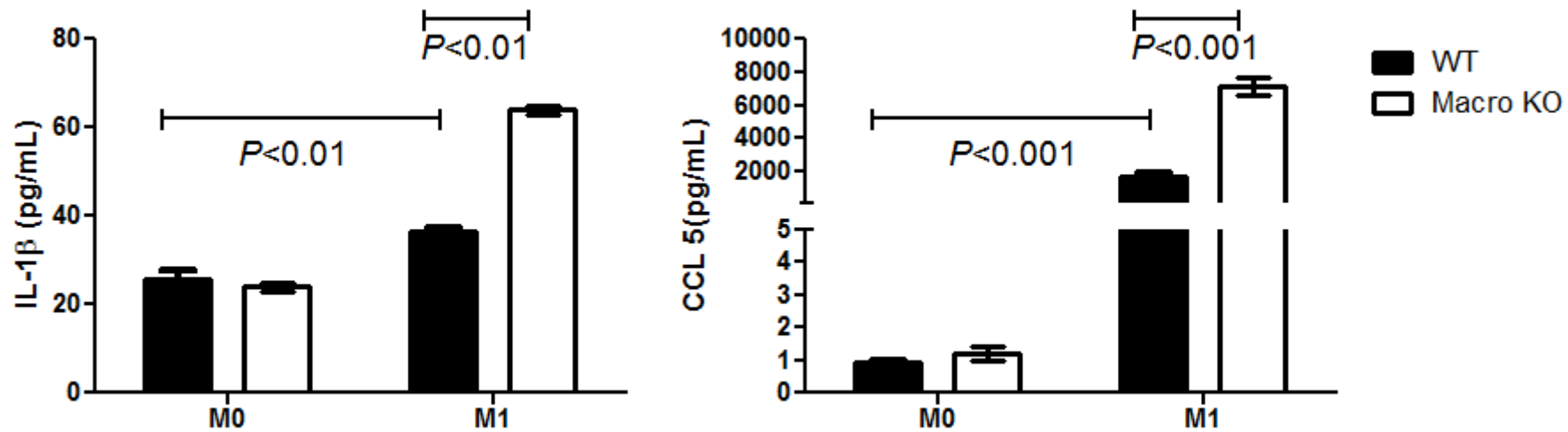


Figure S12. AT_1 receptor-deficient macrophages have augmented cytokine production during M1 differentiation in vitro. Protein levels of IL-1 β and CCL5 measured by ELISA in supernatants from cultures of *WT* and *Macro KO* peritoneal macrophages subjected to M1 stimulation.

S13

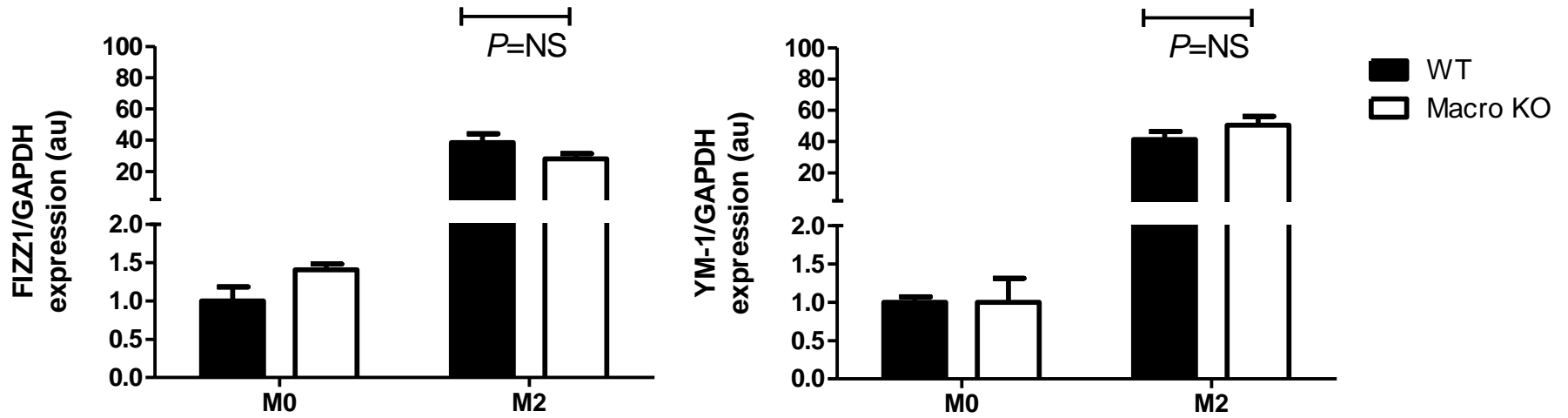


Figure S13. AT_1 receptor on macrophages does not regulate M2 differentiation in vitro. *WT* and *Macro KO* macrophages showed similar mRNA expression of the M2 markers FIZZ1 and YM-1 at baseline (“M0”) and following M2 stimulation for 24 hours with IL-4 (“M2”).

S14

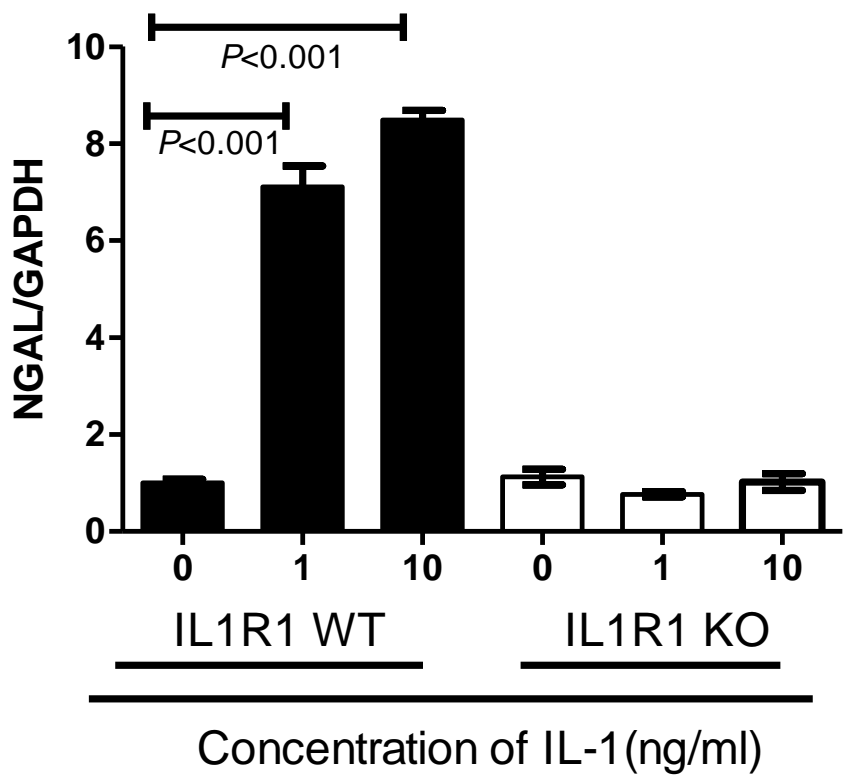
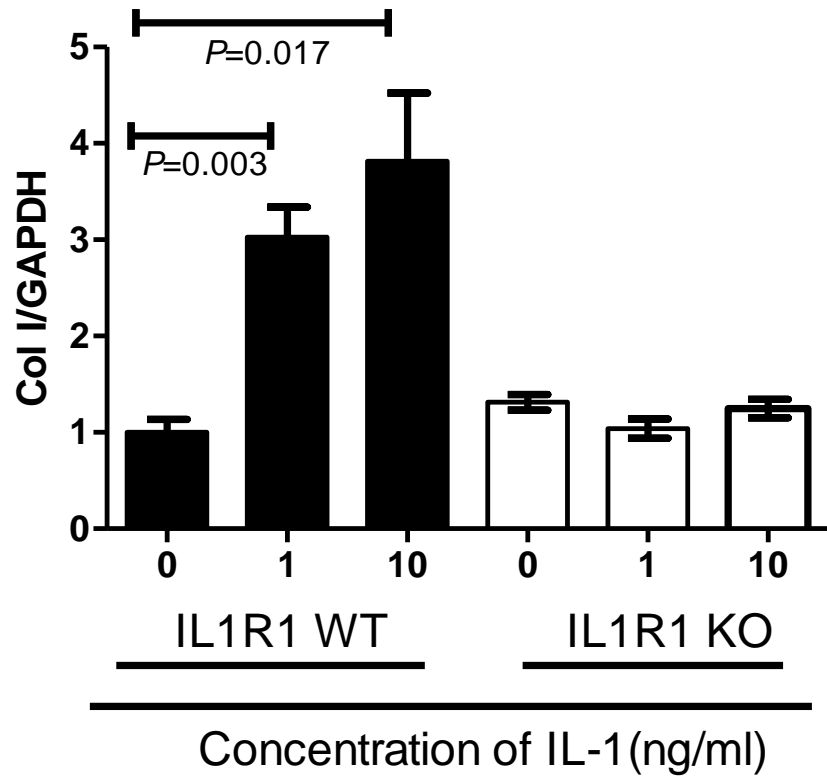
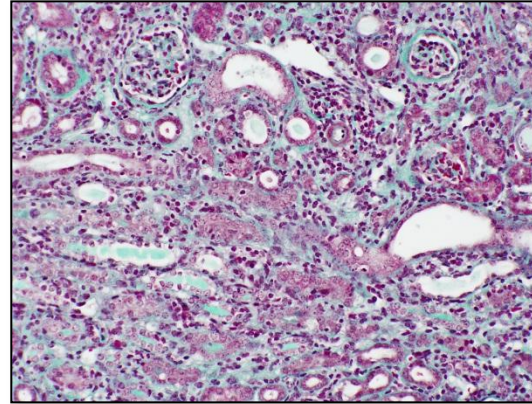
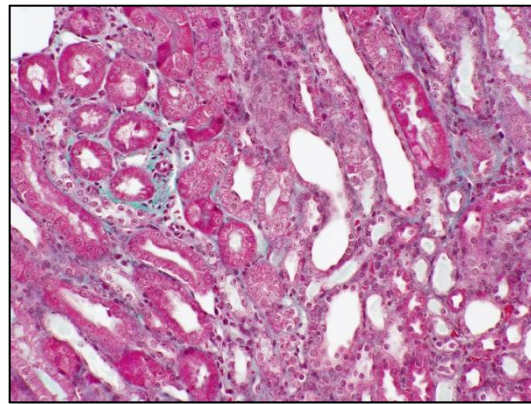


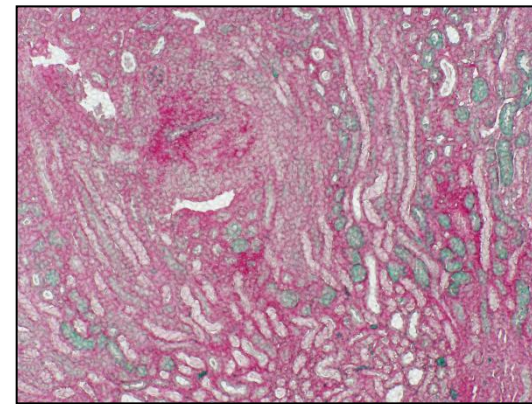
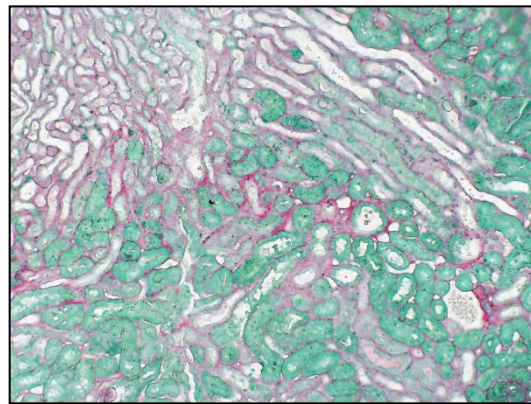
Figure S14. Interleukin-1 induces Collagen I and NGAL in renal tubular cells. Collagen I (“Col I”) and NGAL mRNA expression in wildtype (“IL1R1 WT”) and IL-1 receptor-deficient (“IL1R1 KO”) kidney epithelial cells following 6 hours of stimulation in vitro with Interleukin-1 β .

Supplemental Paragraph 5: Development of kidney cross-transplant UUO model. To precisely define the interactions between infiltrating macrophages and renal parenchymal cells in the pathogenesis of kidney fibrosis, we developed a kidney transplantation-ureteral obstruction (KT-UO) model, the first of its kind to our knowledge. In this model, a kidney is transplanted from a wild-type or IL-1 receptor-deficient (*IL-1R1* KO) mouse into a *Macro WT* or *KO* animal of the same genetic background strain thereby avoiding any graft rejection. Concomitantly, ureteral obstruction is performed on the transplanted kidney to evaluate the contribution of infiltrating macrophages from the kidney recipient to renal fibrosis in the donor kidney. We deemed this surgical strategy preferable to transplanting bone marrow from *Macro WT* and *KO* animals into *IL-1R1 WT* and *KO* recipients because our KT-UO strategy excludes possible confounding, indirect effects of macrophage IL-1 on kidney damage through activation of non-renal IL-1 receptors, such as on other hematopoietic cell lineages (3), and the generation of bone marrow chimeras involves whole body irradiation of the recipient that could separately trigger gene expression programs for kidney fibrosis (4). Nevertheless, despite our considerable experience with kidney cross-transplantation in which we have detected no persistent ischemic renal damage (5), we wanted to confirm that ischemia-reperfusion artifact would not obscure the evolution of obstruction-induced renal fibrosis even 7 days following KT-UO in wild-type cohorts. We found that KT-UO kidneys developed notable fibrosis at 7 days that became severe after 2 weeks (Supplemental Figure S15) as is seen in the standard UUO model.

S15



Masson



**Sirius red/
fast green**

day 7

day 17

Figure S15. Validation of kidney transplant – ureteral obstruction (KT-UO) model. 7 or 17 days following concomitant kidney transplantation and ureteral obstruction, the KT-UO kidney was harvested, sectioned, and stained for Masson trichrome or Sirius red / fast green. In the Masson stain, collagen appears green whereas in the Sirius red / fast green stain, collagen stains red (magnification x20).

Supplemental Paragraph 6: KT-UO transplant groups. Following validation of our KT-UO model, *IL-1R1 WT* or *IL-1R1 KO* kidneys were transplanted into *Macro WT* or *Macro KO* animals (Supplemental Table S2) to quantify the contribution of macrophage-generated IL-1 from the recipient to IL-1 receptor-mediated fibrosis in the donor kidney. *Wild-type* animals had wild-type macrophages and a full complement of IL-1 receptors in the KT-UO kidney. *Macro KO IL-1R1 WT* mice lacked AT_{1A} receptors on macrophages and were transplanted with a wild-type kidney. *Macro WT IL-1R1 KO* mice had wild-type macrophages and an IL-1 receptor-deficient KT-UO kidney. Lastly, *Macro KO IL-1R1 KO* mice lacked AT_{1A} receptors in macrophages and IL-1 receptors in the KT-UO kidney.

S16

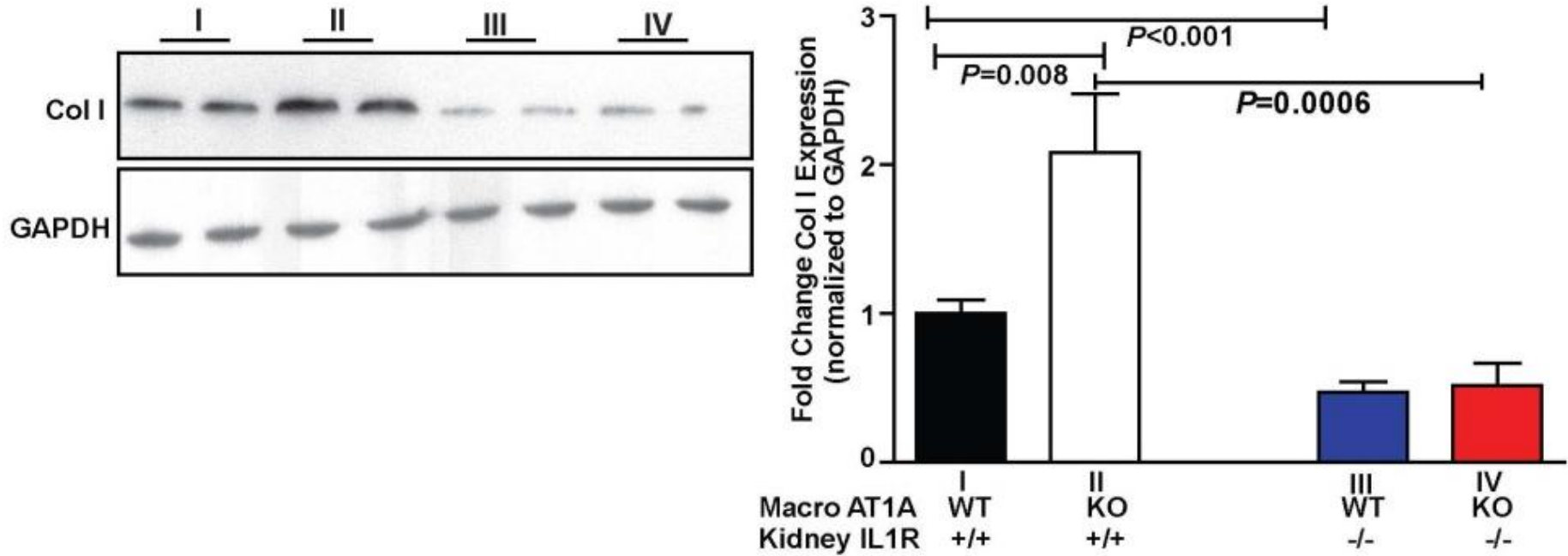


Figure S16. Renal collagen protein content in the kidney transplant – ureteral obstruction (KT-UO) studies. Left, representative western blot for collagen I protein in obstructed kidneys 7 days after KT-UO. Right, quantitation by densitometry. KT-UO groups defined in Table S2 and Supplemental Paragraph 6.

S17

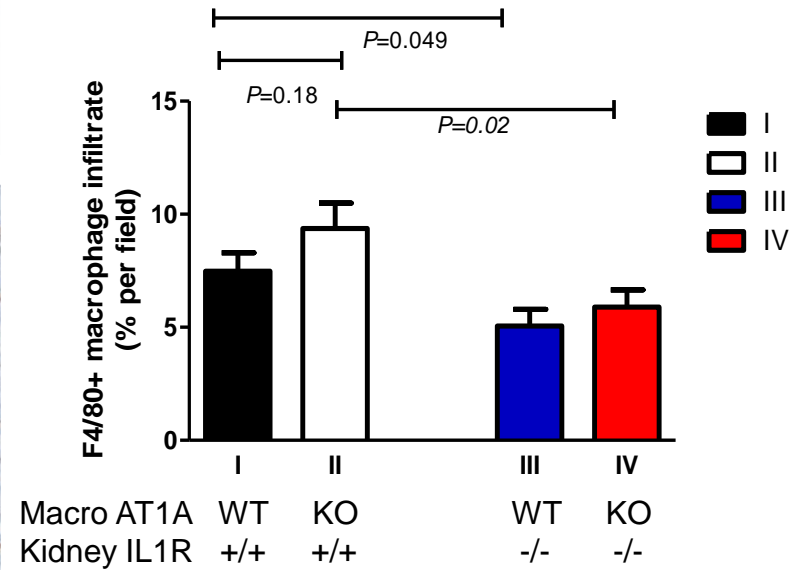
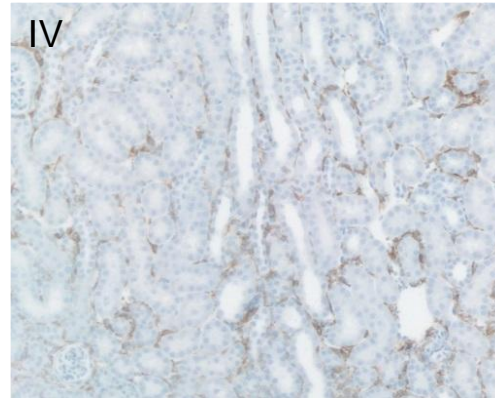
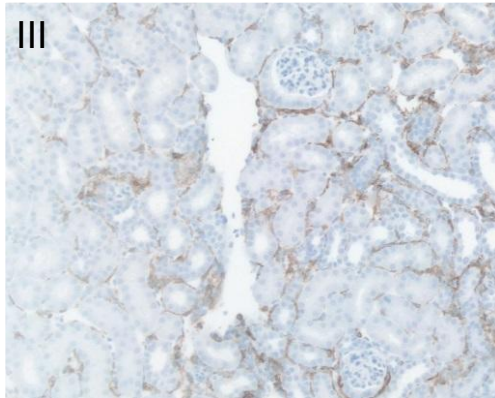
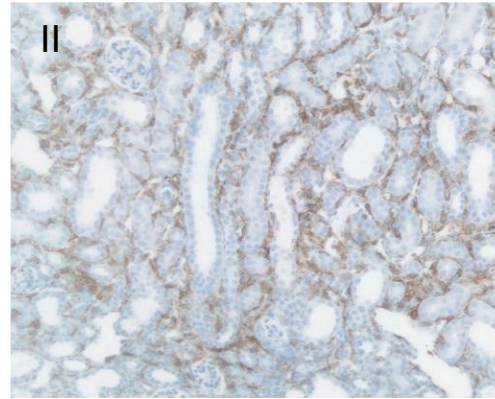
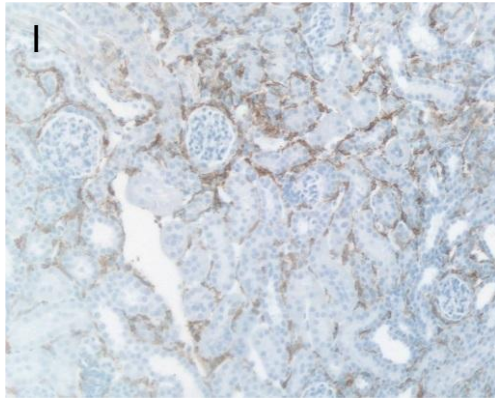


Figure S17. Renal macrophage infiltration in the kidney transplant – ureteral obstruction (KT-UO) studies. Representative sections showing F4/80⁺ macrophage infiltration in KT-UO kidneys at day 7, quantitation on right. (magnification x20).

Table S1. Genes showing differential expression ($p < 0.05$) in CD45⁺CD11b⁺Ly6c^{hi} macrophages from *Macro KO* compared with *WT* obstructed kidneys:

Genes up-regulated in *Macro KO* group

Gene Bank accession no.	Symbol	P-value
Mm00478374	Ptgs2	<0.00001
Mm00443258	Tnf	<0.00001
Mm00448463	Ptprc	<0.00001
Mm00483146	Cd38	<0.00001
Mm00441724	Tgfb1	<0.00001
Mm00437762	B2m	<0.00001
Mm00432050	Bax	<0.00001
Mm00446953	Gusb	<0.00001
Mm00516004	Hmox-1	=0.0001
Mm00441242	Ccl2	=0.0001
Mm00441895	Cd40	=0.0001
Mm00479807	Nfkb2	=0.0001
Mm00476361	Nfkb1	=0.0002
Mm00833995	Ikbkb	=0.0002
Mm00446968	H2Eb1	=0.0003
Mm00444543	Cd86	=0.0009
Mm01302428	Cd5	=0.001
Mm00711660	Cd80	=0.001
Mm00438656	Edn1	=0.001
Mm00434228	Il1b	=0.0012
Mm00434165	Il12	=0.0012
Mm00839636	Cd68	=0.0012
Mm01256734	Fn1	=0.0012
Mm00437858	C3	=0.0012
Mm01160477	Stat6	=0.0012
Mm99999051	Ccr2	=0.0017
Mm00434225	Il18	=0.0023

Mm00782550	Socs1	=0.0033
Mm00432608	Ccr7	=0.0037
Mm00441258	Ccl3	=0.0040
Mm00445235	Cxcl10	=0.0040
Mm00448890	Stat4	=0.0041
Mm00438334	Csf3	=0.0057
Mm00438328	Csf2	=0.0062
Mm00446190	Il6	=0.0087
Mm00440485	Nos2	=0.0121
Mm00439518	Stat1	=0.0137
Mm00439616	Il10	=0.0168
Mm00432688	Csf1	=0.0181
Mm01288992	Il12b	=0.0227
Mm00449197	Vcam1	=0.0266
Mm00434291	Il17	=0.0285
Mm00438259	Cxcr3	=0.0304
Mm00433237	Fas	=0.036
Mm00439620	Il1a	=0.0383
Mm00599683	Cd3e	=0.0466
Mm00442754	Cd4	=0.0496

Genes down-regulated in *Macro KO* group

Gene Bank accession no.	Symbol	P-value
Mm00519283	Cd34	=0.0002
Mm00801606	Col4a5	=0.0020
Mm00437304	Vegfa	=0.0187
Mm00484741	Smad7	=0.04
Mm01187091	Ece1	=0.0466

Table S2. KT-UO experimental groups.

Group	Kidney Donor	Recipient
I = Wild-type	<i>IL-1R1^{+/+}</i>	<i>WT</i>
II = Macro KO IL-1R1 WT	<i>IL-1R1^{+/+}</i>	<i>Macro KO</i>
III = Macro WT IL-1R1 KO	<i>IL-1R1^{-/-}</i>	<i>WT</i>
IV = Macro KO IL-1R1 KO	<i>IL-1R1^{-/-}</i>	<i>Macro KO</i>

Detailed Methods

Mice. C57BL/6 *Agtr1a*^{flox/flox} mice were previously generated (6), backcrossed 6 generations to the 129/SvEv background, and then crossed in 2 steps of breeding with 129/SvEv mice harboring *Cre recombinase* under the control of the *LysM* promoter (1) to yield 129/SvEv *LysM Cre*⁺ *Agtr1a*^{flox/flox} (*Macro KO*) mice and their corresponding *wild-type* (*WT* = *LysM Cre*⁻ *Agtr1a*^{flox/flox}) littermates for experiments. Verification of *Agtr1a* excision was performed on purified immune cell populations and solid organ tissues as described below. To confirm selective *LysM Cre* expression in myeloid cells, *mT/mG* mice from Jackson Laboratory were crossed with the *LysM Cre* transgenic lines. *mT/mG* mice normally express red fluorescence protein in all tissues. When *Cre* is present, the *mT* cassette is deleted, triggering expression of the membrane-targeted *EGFP* (2). IL-1 receptor-deficient (*IL-1R1 KO*) mice on the C57BL/6 background were purchased from Jackson Laboratory and backcrossed to the 129/SvEv strain for 6 generations to increase susceptibility to kidney damage. Thereafter, 129/SvEv *IL1R1* heterozygotes were intercrossed to yield the *IL1R1 KO* and *WT* littermates for our experiments. Eight- to 12-week-old male mice were used for experiments.

Unilateral ureteral obstruction model of kidney fibrosis. Unilateral ureteral obstruction (UUO) was executed as described previously (7). Briefly, after inhaled anesthesia, the left ureter was isolated and ligated 3-5 mm below its origin. 3 or 7 days following surgery, mice were sacrificed, and the obstructed and contralateral non-obstructed kidneys were harvested for analysis. Losartan-treated mice received a dose of 30mg/kg/d (8) diluted in the drinking water beginning 72 hours prior to UUO and continuing until organ harvest on day 7 of UUO. The losartan was provided by Merck as a gift.

Histological analysis for UUO. Portions of kidney were fixed and pathological analysis was performed as described previously (9). Paraffin sections (5µm thick) were stained with picosirius red for detecting total collagen. To evaluate the number of collagen-producing myofibroblasts, slides were stained with an antibody to α -smooth muscle actin (#5694, Abcam) at a 1:400 dilution. To assess macrophage infiltration in

the kidneys, sections were stained with anti-F4/80 (#MCA497G, Serotec), according to the manufacturer's instructions. On each section, 20 randomly selected fields were then digitally photographed and scored in a blinded fashion via computerized morphometric analysis. Areas of positive signals were quantified by using a computer-assisted color-image-analysis system (Image J 1.38 for windows at <http://rsb.info.nih.gov>). Scores were averaged for each animal, and then for each group. Picrosirius red-stained slides were examined under polarized microscopy.

Western blots for collagen I. Kidney tissues (10mg) were homogenized in RIPA buffer (#9806, Cell Signal). Concentration of protein was quantitated by the Bradford method (#23236, Thermo Scientific). Equal amounts of sample were subjected to electrophoresis through 4-12%Bis-Tris Gels and transferred to PVDF membranes (#IB401002, Life technologies). After blocking with 5% milk in TBS, the blots were incubated with anti-mouse collagen type I antibody (1:500, #AB765P, Millipore) or anti-mouse GAPDH (1:10,000, #MAB374, Millipore) overnight in 4°C. The blots were then washed and incubated for 1 hour at room temperature with individual secondary antibodies accordingly. Bands were detected using an enhanced chemiluminescence detection system (#RPN2108, GE Health). After exposure to Carestream Kodak film (#F5513-50EA, Sigma-Aldrich), the developed graphs were scanned and quantified by densitometry through Image J 1.38 for windows (10).

Confocal immunofluorescence microscopy. To examine the spatial distribution of M1 and M2 macrophages in the kidney, we performed immunofluorescence double staining for iNOS (M1) or CD206 (M2) markers with the pan-macrophage marker F4/80. Briefly, frozen kidney sections were processed with 4% paraformaldehyde for iNOS staining or PBS for CD206 staining, and then stained with anti-mouse iNOS Ab (1:100, #ABN26, Millipore) or anti-CD206 Ab (1:100, #C086C2, Biolegend), followed by Alexa Fluor 568 goat-anti-rabbit Ab (1:500, #A11036, Life Technologies) or Alexa Fluor 594 goat-anti-rat Ab (1:500, #A11007, Life Technologies). Next, we stained the sections with FITC-conjugated anti-mouse F4/80 antibody (1:200, MCA497F, AbD Serotec). The numbers of F4/80⁺ iNOS⁺ cells and F4/80⁺ CD206⁺ cells were counted in 8-10 fields (20X) per slide by an observer masked to experimental conditions. Confocal images

were captured using an LSM 510 Meta DuoScan microscope (Zeiss) and processed using LSM 5 software, version 4.2 (11-13).

Chronic angiotensin II infusion model of hypertension. Experimental animals underwent left nephrectomy to render the remaining kidney more susceptible to damage (9). 1 week later, a pressure-sensing catheter (TA11PA-C10, Transoma Medical) was implanted via the left common carotid artery as described (5). After allowing 7 days for reestablishment of diurnal blood pressure variation, baseline blood pressure measurements were recorded for 3 days by radiotelemetry (Transoma) in conscious unrestrained animals. Then an osmotic mini-pump (ALZET model, 2004) was implanted subcutaneously to infuse Ang II (1000ng/kg/min; Sigma; n≥14 mice per group) or saline (n=4 mice per group) continuously for 28 days. Kidneys were then harvested as described above and fixed for Masson trichromatic staining. Glomerulosclerosis, interstitial fibrosis, and tubular cell reactivity, dilation, and casts were scored by a pathologist masked to experimental conditions using a semi-quantitative scoring system as follows: 0 – none, 1 – minimal, 2 – mild, 3 – moderate, and 4 – moderately severe (9).

Isolation of spleen cells. To examine *Agtr1a* gene expression in lymphocyte populations, murine splenocytes were isolated as previously described (14), then counted, and re-suspended in FACS buffer. Cells were stained with PE-labeled anti-CD3, APC-labeled anti-CD19 (BD Bioscience), PE-labeled anti-Thy1.1, and FITC-labeled anti-F4/80 (Serotec) and corresponding isotype antibodies without fixation, and then sorted immediately in the Flow Cytometry Facility at Duke University as described (15).

Isolation of RNA and real-time PCR. Total RNA was isolated from individual cells or tissues by using the RNeasy Mini Kit according to the manufacturer's instructions. RNA expression levels were then determined for *Agtr1a* as described (5) and for IL-1 α , IL-1 β , TNF- α , IL-10, IL-12a (IL-12 p35), IL-12b (IL-12 p40), IL-1R1, IL-1R2, YM-1, FIZZ-1, Arg-1, CCL2, CCL5, NGAL, PAI-1, TGF- β , *Agtr1b*, and Col I using TaqMan primers (Applied Biosystems) in real-time PCR, as described (15).

Peritoneal macrophage isolation and treatment. Peritoneal macrophages were harvested from naive mice 4 days after an i.p. injection of 3% thioglycollate as previously described (15) and then suspended in FACS buffer for fluorescent cell

sorting using FITC-labeled anti-F4/80 as above to maximize the purity of the macrophage preparation (99%), or placed in R10 complete medium for in vitro culture experiments. Classical macrophage activation converting M0 macrophages to the pro-inflammatory M1 phenotype was executed following a previously described protocol (16). Briefly, isolated peritoneal macrophages were rested for 3 hours and then pre-conditioned with 150 IU/ml IFN- γ (Invitrogen, 4031) for 6 hours and then stimulated with 100 ng/ml LPS (Sigma, L2630) for 18 hours. To accomplish M2 differentiation, macrophages were incubated with 5 ng/ml IL-4 (R&D Systems, RM IL-4 CF) for 24 hours as described (17).

Primary culture of mouse renal tubular cells. Primary mouse renal tubular cells were obtained and cultured by following a previously described method (18). Briefly, 129/SvEv male mice aged 4-6 weeks were anesthetized and flushed with 5 mL ice-cold HBSS (Gibco,14175095). Renal cortices were dissected visually and sliced into small pieces. The fragments were transferred through two layers of nylon sieves (pore size 125 μ m and 106 μ m, VWR 57334-184 and 57334-186). After sieving, mouse tubular fragments were selected and seeded in collagen pre-coated flasks (Corning) with Dulbecco's modified Eagle's/Ham's F12 (DMEM-F12) (Gibco,11039-021), in the presence of 10% heat inactivated FBS (Gibco,10099-147), 1% L-glutamine, and 1% penicillin/streptomycin. The plate was incubated in a standard humidified incubator equipped with 5% CO₂. The medium was changed two days later and maintained every other day until the monolayer of cells reached 90% confluence. Immunostaining against megalin (SC-16478, Santa Cruz) confirmed the presence of tubular cells. For the IL-1 stimulation assays, renal tubular cells were cultured with Interleukin-1 β (R&D Systems, 401-ML/CF) for 6 hours at 37°C.

Co-culture of activated macrophages and mouse renal tubular cells. For co-culture experiments, freshly isolated peritoneal macrophages were first seeded on transwell inserts (BD,353502), and either maintained in M0 conditions or classically activated to M1 phenotype as described above. Then these inserts were placed into another transwell companion plate coated with quiescent mouse renal tubular cells. After co-culture for 6 hours, RNA was harvested specifically from the renal tubular cells in the plate's lower chamber.

Isolation of macrophages directly from kidneys. Kidneys were harvested and minced, followed by incubation with 0.1% collagenase type I (Gibco,17100-017) for 40 min at 37°C. Single cell suspensions were obtained by filtering through a 40µm cell strainer. Thereafter, cells were stained with fluorescently-labeled anti-CD45, anti-CD11b, and anti-Ly6c (BD Bioscience), and subjected to fluorescent cell-sorting. The gating strategy was as follows: 1st gate on single cells, 2nd gate on CD45⁺ cells, 3rd gate on CD11b⁺ cells. Cells meeting these criteria were then separated by Ly6c high or low staining and saved for real-time PCR or microarray analysis.

Microarray analysis of macrophages infiltrating the kidney. As described above, CD45⁺CD11b⁺Ly6c^{hi} macrophages were isolated from obstructed kidneys of *Macro KO* and *WT* mice 7 days after UO. RNA was then harvested and reverse-transcribed to cDNA, which was subjected to quantitative PCR in a 92-gene Taqman Immune Array (Applied Biosystems; n=4 per group) as described previously (19).

Cytokine ELISA. Thioglycollate-induced macrophages were obtained and conditioned as described above. Supernatants from LPS- or vehicle-treated macrophages were collected following 24 hours of stimulation. Cytokines were quantified in the supernatants by using ELISA Kits from Invitrogen according to the manufacturer's instructions.

Model of kidney transplantation-ureter obstruction (KT-UO). To explore the role of cytokines released by infiltrating macrophages in directing kidney damage, we developed a model of kidney transplantation-ureteral obstruction (KT-UO). Briefly, animals were anesthetized, and the donor kidney and ligated ureter were harvested. Renal vessels were anastomosed to the recipient abdominal aorta and vena cava, respectively, below the level of the native renal vessels. The left native kidney was removed at the time of transplant. The transplanted-obstructed kidney and right native "unobstructed contralateral" kidney were harvested 7 or 17 days after the operation as described above. In pilot experiments, Sirius red / fast green and Masson trichromatic staining were performed to visualize kidney fibrosis and damage (Supplemental Figure S15).

Statistics. The values of each parameter within a group are expressed as the mean ± the standard error of the mean (SEM). For comparisons between groups with

normally distributed data, statistical significance was assessed using ANOVA or two-tailed unpaired student's *t* test. For comparisons between groups with non-normally distributed variables, a Wilcoxon test was employed.

Acknowledgements

This work was supported by funding from the Medical Research Service of the Veterans Administration, National Institutes of Health Grant DK087893-03, the Edna and Fred L. Mandel Center for Hypertension and Atherosclerosis Research, the Duke O'Brien Center for Kidney Research, and an American Heart Association Post-doctoral Fellowship. MAS is funded by a Career Development Award BXIK2BX002240 from the Department of Veterans Affairs, Biomedical Laboratory Research and Development Service. Some of the histologic analysis was carried out by the Animal Pathology core facility of the Duke School of Medicine and the Duke Cancer Institute.

References

1. Clausen BE, Burkhardt C, Reith W, Renkawitz R, and Forster I. Conditional gene targeting in macrophages and granulocytes using LysMcre mice. *Transgenic Res.* 1999;8(4):265-77.
2. Muzumdar MD, Tasic B, Miyamichi K, Li L, and Luo L. A global double-fluorescent Cre reporter mouse. *Genesis.* 2007;45(9):593-605.
3. Kuno K, and Matsushima K. The IL-1 receptor signaling pathway. *Journal of Leukocyte Biology.* 1994;56(5):542-7.
4. Brown NJ, Nakamura S, Ma L, Nakamura I, Donnert E, Freeman M, Vaughan DE, and Fogo AB. Aldosterone modulates plasminogen activator inhibitor-1 and glomerulosclerosis in vivo. *Kidney Int.* 2000;58(3):1219-27.
5. Crowley SD, Gurley SB, Oliverio MI, Pazmino AK, Griffiths R, Flannery PJ, Spurney RF, Kim HS, Smithies O, Le TH, et al. Distinct roles for the kidney and systemic tissues in blood pressure regulation by the renin-angiotensin system. *J Clin Invest.* 2005;115(4):1092-9.
6. Gurley SB, Riquier-Brison AD, Schnermann J, Sparks MA, Allen AM, Haase VH, Snouwaert JN, Le TH, McDonough AA, Koller BH, et al. AT1A angiotensin receptors in the renal proximal tubule regulate blood pressure. *Cell Metab.* 2011;13(4):469-75.
7. Chevalier RL, Forbes MS, and Thornhill BA. Ureteral obstruction as a model of renal interstitial fibrosis and obstructive nephropathy. *Kidney Int.* 2009;75(11):1145-52.
8. Crowley SD, Vasievich MP, Ruiz P, Gould SK, Parsons KK, Pazmino AK, Facemire C, Chen BJ, Kim HS, Tran TT, et al. Glomerular type 1 angiotensin receptors augment kidney injury and inflammation in murine autoimmune nephritis. *J Clin Invest.* 2009;119(4):943-53.
9. Crowley SD, Frey CW, Gould SK, Griffiths R, Ruiz P, Burchette JL, Howell DN, Makhanova N, Yan M, Kim HS, et al. Stimulation of lymphocyte responses by angiotensin II promotes kidney injury in hypertension. *Am J Physiol Renal Physiol.* 2008;295(2):F515-24.
10. Anders HJ, Vielhauer V, Frink M, Linde Y, Cohen CD, Blattner SM, Kretzler M, Strutz F, Mack M, Grone HJ, et al. A chemokine receptor CCR-1 antagonist reduces renal fibrosis after unilateral ureter ligation. *J Clin Invest.* 2002;109(2):251-9.
11. Iwata Y, Bostrom EA, Menke J, Rabacal WA, Morel L, Wada T, and Kelley VR. Aberrant macrophages mediate defective kidney repair that triggers nephritis in lupus-susceptible mice. *J Immunol.* 2012;188(9):4568-80.
12. Wang H, Gomez JA, Klein S, Zhang Z, Seidler B, Yang Y, Schmeckpeper J, Zhang L, Muramoto GG, Chute J, et al. Adult renal mesenchymal stem cell-like cells contribute to juxtaglomerular cell recruitment. *J Am Soc Nephrol.* 2013;24(8):1263-73.
13. Lin SL, Castano AP, Nowlin BT, Lopher ML, Jr., and Duffield JS. Bone marrow Ly6Chigh monocytes are selectively recruited to injured kidney and differentiate into functionally distinct populations. *J Immunol.* 2009;183(10):6733-43.

14. Nataraj C, Oliverio MI, Mannon RB, Mannon PJ, Audoly LP, Amuchastegui CS, Ruiz P, Smithies O, and Coffman TM. Angiotensin II regulates cellular immune responses through a calcineurin-dependent pathway. *J Clin Invest*. 1999;104(12):1693-701.
15. Crowley SD, Song YS, Sprung G, Griffiths R, Sparks M, Yan M, Burchette JL, Howell DN, Lin EE, Okeiyi B, et al. A role for angiotensin II type 1 receptors on bone marrow-derived cells in the pathogenesis of angiotensin II-dependent hypertension. *Hypertension*. 2010;55(1):99-108.
16. Edwards JP, Zhang X, Frauwirth KA, and Mosser DM. Biochemical and functional characterization of three activated macrophage populations. *J Leukoc Biol*. 2006;80(6):1298-307.
17. Usher MG, Duan SZ, Ivaschenko CY, Frieler RA, Berger S, SchÄ¼tz Gn, Lumeng CN, and Mortensen RM. Myeloid mineralocorticoid receptor controls macrophage polarization and cardiovascular hypertrophy and remodeling in mice. *The Journal of Clinical Investigation*. 2010;120(9):3350-64.
18. Terryn S, Jouret F, Vandenabeele F, Smolders I, Moreels M, Devuyst O, Steels P, and Van Kerkhove E. A primary culture of mouse proximal tubular cells, established on collagen-coated membranes. *Am J Physiol Renal Physiol*. 2007;293(2):F476-85.
19. Zhang JD, Patel MB, Song YS, Griffiths R, Burchette J, Ruiz P, Sparks MA, Yan M, Howell DN, Gomez JA, et al. A novel role for type 1 angiotensin receptors on T lymphocytes to limit target organ damage in hypertension. *Circ Res*. 2012;110(12):1604-17.